Hindawi
Shock and Vibration
Volume 2020, Article ID 4289281, 20 pages
https://doi.org/10.1155/2020/4289281

Review Article

A Review on Model and Control of Electromagnetic Active Engine Mounts

Henghai Zhang,[1,2] **Wenku Shi**,[1] **Jun Ke**,[3] **Guoyu Feng**,[4] **Junlong Qu**,[1] **and Zhiyong Chen**[1]

[1]*State Key Laboratory of Automotive Simulation and Control, Jilin University, Changchun 130022, China*
[2]*School of Automotive Engineering, Shandong Jiaotong University, Jinan 250023, China*
[3]*Zhejiang Provincial Key Laboratory of Modern Textile Machinery, Zhejiang Sci-tech University, Hangzhou 310018, China*
[4]*School of Aviation Operations and Services, Aviation University of Air Force, Changchun 130022, China*

Correspondence should be addressed to Henghai Zhang; zhanghh13@mails.jlu.edu.cn and Zhiyong Chen; chen_zy@jlu.edu.cn

Received 21 December 2019; Accepted 5 February 2020; Published 22 June 2020

Academic Editor: Mohammad Rafiee

The isolation of the body from engine vibration is the most challenging and disruptive vibrational problem. Active engine mounts (AEMs), especially electromagnetic AEMs, achieve a significant performance improvement in decreasing the wide frequency band vibration. Increasing research interest is necessary to provide the academic community with a guideline for electromagnetic AEMs. Therefore, the current review aims to comprehensively supplement the review of AEMs. The key reviews of electromagnetic AEMs focus on (1) general considerations of electromagnetic AEMs, (2) models, and (3) control strategies. This paper presents a review of the current status and developmental progress of AEMs. A theoretical model, a finite-element model, and the identification (or experimental modelling) of electromagnetic AEMs during the last 2 decades are then studied. Finally, control strategies, such as classical control, adaptive control, and two degree of freedom (2DOF) control, are discussed and compared. The main purpose of this paper is to meet the needs of researchers and engineers engaged in electromagnetic AEM analysis and control.

1. Introduction

To meet the requirements of low emissions and low fuel consumption, downsizing, on-demand cylinders (COD), turbochargers, and active fuel management are applied in vehicles [1–5], which results in changes in the engine vibration excitation level and dominant engine order shown in Figures 1(a) and 1(b). Attenuation of the vibration from the engine is the most challenging and disruptive vibrational problem. Compared with passive engine mounts or semi-active engine mounts, the active engine mount (AEM) achieves significant noise, vibration, and harshness (NVH) performance improvements [5, 6]. The actuator is the key component of the AEM. Different actuators, such as the pneumatic actuator [7–23], the magnetostrictive actuator [24, 25], the piezoelectric actuator [26–49], and the electromagnetic actuator [4, 50], have been applied to AEMs by scholars and researchers. This present work is focused on an AEM with an electromagnetic actuator, named the electromagnetic AEM. The electromagnetic AEM has attracted the attention of suppliers and automobile manufacturers. Researchers from Avon VMS [4, 51–53], Continental [1, 54, 55], Nissan [56, 57], Isuzu [58–60], Honda [61], Hyundai Motor [62–66], Paulstra [49, 67], and GM [68] have successively studied electromagnetic AEMs with a conventional passive hydraulic engine mount (HEM) extended by an electromagnetic actuator.

One of the main objectives of the present work is to summarize and show general information about the model of AEMs. Models can be categorized as theoretical models, finite-element models, and identification [1], which can provide deep comprehension of the dynamic behaviour of

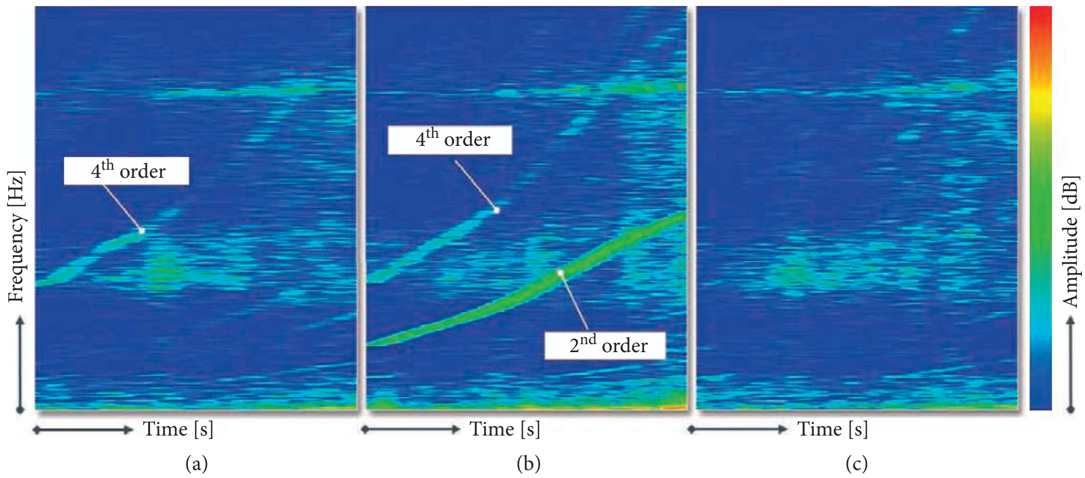

Figure 1: Vibration results of 8-cylinder mode and 4-cylinder mode in driving mode with AEM off or on [5]: (a) 8-cylinder mode; (b) 4-cylinder mode; (c) 4-cylinder mode AEM on.

AEMs and improve the control performance in designing AEM controllers. A second aim of this present work is a quantitative comparison of the various control strategies of AEMs regarding their weighting functions, the order of controllers, the sampling frequency, and the step size filter length. Based on this comparison, the merits and weaknesses are discussed. The goal is to identify the focus of the literature on the dynamic modelling and control of AEMs.

This article is organized as follows: General Considerations of Electromagnetic AEMs relates the main considerations and parameters needed for a deep comprehension of AEMs. Model describes a review of the different models of AEMs: Section 3.1 reviews the theoretical model, Section 3.2 reviews the finite-element model, and Section 3.3 reviews identification (or the experimental model). In Control Strategies, classical control problems of AEMs are discussed, and adaptive control, such as LMS, filtered-x least mean squares, minimal controller synthesis (MCS), robust control, and 2DOF control, are reviewed. Finally, concluding remarks are presented in Conclusions.

2. General Considerations of Electromagnetic AEMs

2.1. Actuator. Electromagnetic actuators, such as solenoids or voice coil (moving coil) actuators, are shown in Figure 2 and have the characteristics of compact structure, low energy consumption, sensitive response, work densities, easily control, and good force.

2.1.1. Electromagnetic AEMs with a Voice Coil Actuator. The passive HEM and the voice coil actuator are designed as the passive components and the active components of the electromagnetic AEM, respectively. The voice coil actuator produces the dynamic force and drives the upper chamber or the lower chamber of the AEM. As shown in Figure 3, Fursdon et al. [51] developed an electromagnetic AEM, which is installed on the Audi S8 [4]. The dynamic force of the actuator drives the main fluid chamber of AEM. Vahdati and Heidari [69] proposed an engine mounting design. The dynamic force of the actuator drives the compensation chamber of the AEM.

2.1.2. Electromagnetic AEM with a Solenoid Actuator. The coil of the solenoid actuator generates a magnetic field, which attracts the iron component to the coil [50]. Similar to the structure of the electromagnetic AEM with a voice coil actuator, the passive HEM and the solenoid actuator are designed as the passive components and active components of the electromagnetic AEM with a solenoid actuator, respectively. As shown in Figure 4, the excitation plate is actuated by the solenoid actuator, which changes the liquid pressure of the chamber. Mansour et al. [71–73] proposed an electromagnetic AEM with a solenoid actuator. The solenoid actuator is placed on the inertia track plate of the HEM, and the passive structure of the HEM is retained. Continental [54, 55] developed an electromagnetic AEM with a solenoid actuator for testing on vehicles. The electromagnetic AEM with a solenoid actuator shown in Figure 4 was applied on the Honda INSPIRE [61, 70, 74]. Kitayama et al. [75–83] studied the linear electromagnetic actuator for AEM. The permanent magnet is bonded on a diaphragm. A magnetic field is produced by the electric current in the solenoid coil, which can produce mechanical force and alter the pressure of fluid in the chamber [84].

From the above discussion, the passive HEM and actuator are designed as the passive components and active components of the electromagnetic AEM, respectively. The voice coil actuator subsystem consists of a permanent magnet and a coil, as shown in Figure 5; the electrical differential equation of voltage applied on the voice coil actuator can be expressed as

$$u(t) = K_M \dot{x}_a(t) + Ri(t) + L\frac{\mathrm{d}i(t)}{\mathrm{d}t}, \quad (1)$$

where $u(t)$, R, L, and $x_a(t)$ are the input voltage applied on the voice coil, the electrical resistance of the voice coil, the

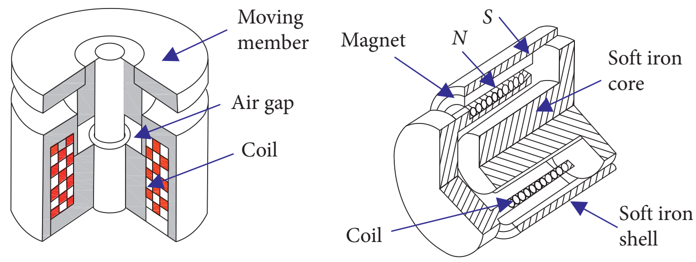

(a) (b)

Figure 2: Electromagnetic actuators [50]: (a) solenoid; (b) voice coil actuator.

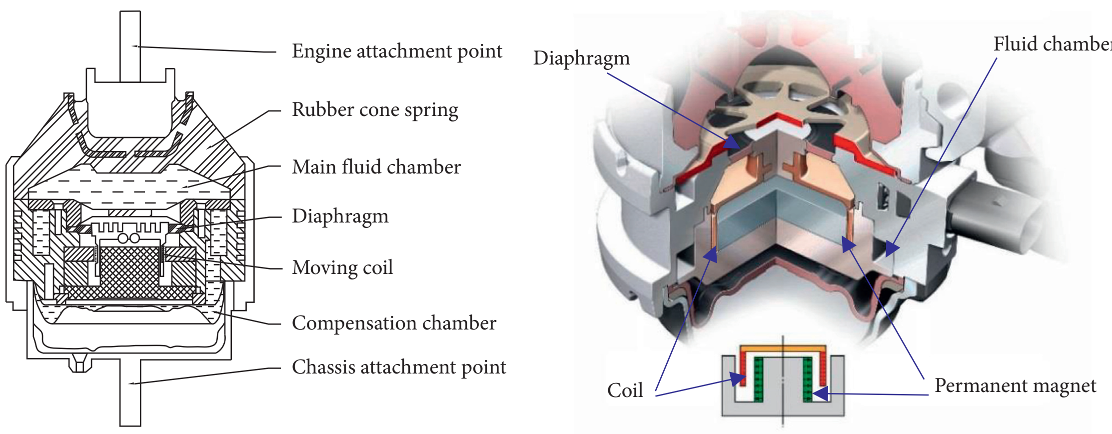

(a) (b)

Figure 3: Electromagnetic AEM with a voice coil actuator: (a) AEM with a voice coil [51]; (b) AEM with a voice coil on the Audi S8 [4].

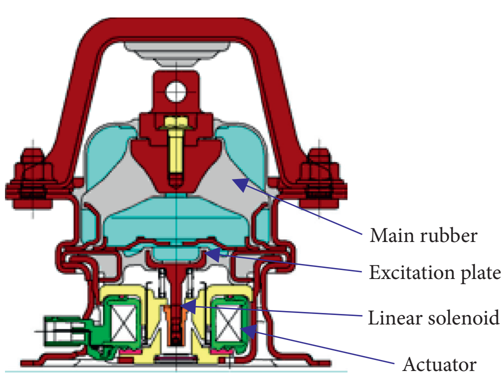

Figure 4: AEM working with a solenoid [61, 70].

inductance of the voice coil, and the position of the moving diaphragm, respectively.

The magnetic flux generated by the permanent magnet interacts with the current in the coil, and the actuator produces a Lorentz force, which can be expressed as

$$F = Bl_w i, \tag{2}$$

where B, l_w, and i denote the field density, wire length, and current flowing in the wire, respectively.

The decoupling membrane of the HEM is replaced by the voice coil actuator or the solenoid actuator. The actuator acting on the diaphragm is usually regarded as a mass-spring-damper system, as shown in Figure 6, which can be expressed by

$$\begin{aligned} f_a(t) - p_u(t)A_a = {} & m_a\ddot{x}_a(t) + d_a(\dot{x}_a(t) - x_c(t)) \\ & + k_a(x_a(t) - x_c(t)), \end{aligned} \tag{3}$$

where f_a is the actuator force, p_u is the pressure inside the upper fluid chamber, m_a is the actuator mass, d_a is the damping coefficient of the actuator, and k_a is the spring constant of actuator. When the actuator is turned on, the displacement of the chassis is small. If it is supposed that the chassis is fixed, then $x_c(t)$ is zero.

2.2. Fluid. The fluid in an AEM is assumed to be incompressible. The continuity equation of the upper chamber is expressed as

$$A_i x_i(t) + A_a(x_a(t) - x_c(t)) = A_m(x_e(t) - x_c(t)) + \Delta V_b, \tag{4}$$

where A_a, A_i, and A_m denote the actuator diaphragm area, the cross-sectional area of the inertia track, and the equivalent piston area of the main rubber spring, respectively. x_a, x_i, x_e, and x_c denote the displacement of the actuator, the fluid in the inertia track, the AEM at the engine side, and the AEM at the chassis side, respectively. The volumetric compliance element is expressed as

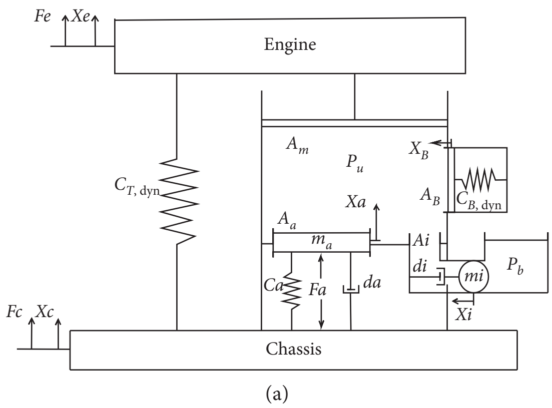

FIGURE 5: Lumped parameter model of an AEM with a voice coil [85]: (a) lumped parameter model; (b) circuit of voice coil actuator.

$$C_b = \frac{\Delta V_b}{P(t)}. \tag{5}$$

Frequency-dependent stiffness and damping of the fluid are generated in the inertia track of the HEM [86]. The static pressure of the AEM upper chamber is relieved only in the inertia track [65]. A column of fluid is created in the inertia track. The friction generated by the fluid flow in the track is not directly transmitted to the chassis. The inertia track is assumed to be connected to the absolute reference frame [66]. The fluid in the inertial track is forced to flow by the pressure in the upper chamber, which can be represented by

$$-p_u(t)A_i = m_i\ddot{x}(t) + d_i\dot{x}_i(t) + k_i x_i(t), \tag{6}$$

where m_i and d_i are the equivalent mass and damping coefficient of the fluid in the inertia track, respectively. The stiffness of the lower chamber is smaller than that of the upper chamber [87–89], and the stiffness of the lower chamber k_i can be neglected.

2.3. Elastomeric. The AEM can be designed by incorporating a conventional passive HEM [88–92] with the actuator. The dynamic stiffness of a passive engine mount depends on the frequency, temperature, amplitude, and types of external excitation [93, 94]. Meanwhile, the main rubber spring or elastomer rubber element of the passive engine mount has amplitude- and frequency-related behaviours [95]. The damping, stiffness, and bulking properties of the main rubber spring or elastomer rubber element of the AEM contribute substantially to the dynamic characteristics of the AEM. The frequency-dependent dynamics model of the elastic coupling unit can be traced back to the 18th century; Maxwell et al. studied the behaviour of viscoelastic materials [96]. Some viscoelastic material models have been widely used in simulations, such as the Maxwell [97] and Kelvin–Voigt models [98]. In the AEM mathematical model, the main rubber springs or elastomeric rubber elements are typically modelled using linear spring elements [99, 100] or a spring in parallel to a damper (the Kelvin–Voigt model shown in Figure 6(a)) [101–103], which overestimates both stiffness and damping at higher frequencies.

To settle the problem of the Kelvin–Voigt model, as shown in Figure 6(b), the main rubber spring and its bulking properties are modelled as one spring in parallel to two dampers and another spring. Lambertz et al. [104–108] applied this approach in studying conventional HEMs, and the transfer function of the elastomer element in the Laplace domain is expressed as

$$K_{\text{dyn}}(s) = \frac{F_{(s)}}{X_{(s)}} = k_1 + \frac{d_1k_2s + d_1d_2s^2}{k_2 + (d_1 + d_2)s}, \tag{7}$$

where $K_{\text{dyn}}(s)$ is the dynamic properties of the main rubber spring or elastomer rubber. The damping and stiffness of the high frequency simulation are in good agreement with those of the test [85]. The Kelvin–Voigt model is consistent with the measured loss angle at only one design frequency [109].

2.4. Force Transmitted to the Engine and the Chassis. The force transmitted to the engine, chassis, and body through the AEM, $F_e(t)$, and $F_c(t)$, respectively, can be represented by

$$\begin{aligned} F_e(t) &= -k_r(x_e(t) - x_c(t)) + p_u(t)A_m, \\ F_c(t) &= k_r(x_e(t) - x_c(t)) - p_u(t)(A_m - A_a) \\ &\quad + d_a(\dot{x}_a(t) - x_c(t)) + k_a(x_a(t) - x_c(t)) - f_a(t). \end{aligned} \tag{8}$$

Similar equations [66, 85, 110] are used to deduce the transfer functions to study the dynamic characteristics of electromagnetic AEMs.

3. Model

As discussed in Section 2, the dynamic behaviour of AEMs is nonlinear. Accurate AEM models can improve the controller performance in designing model-based controllers and facilitate the accurate study of the dynamic behaviour of AEMs [111–114]. There are three general models, namely, theoretical models, finite-element models, and identification [1]. The theoretical model is obtained by applying methods from calculus to equations derived from physics. The finite-element models make use of a virtual development

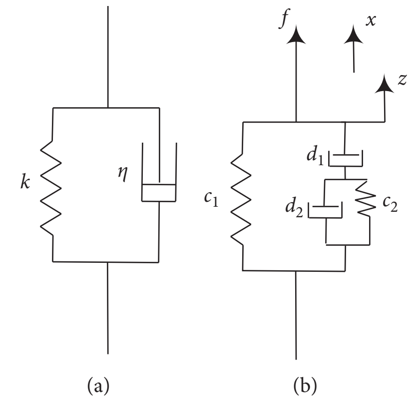

Figure 6: Model of the main rubber spring [85]: (a) Kelvin–Voigt model; (b) model.

environment, such as ADAMS. Identification, which is also named experimental models, is a mathematical model derived from measurements.

3.1. Theoretical Model. The theoretical model describes the dynamic characteristics of the AEM, which is expressed by the transmission performance of force between the chassis and the engine, and the secondary path transfer function of the AEM between the actuator input signal and the output force (displacement or acceleration) on the chassis (or engine) side. It is generally assumed that (1) the forces transmitted to the engine and the chassis are always equal to each other, (2) the displacement or acceleration of the chassis is zero, (3) the stiffness or damping of the elastomeric rubber is independent of the frequency or preload, and (4) the dynamics of the chassis or the mass of the engine are ignored, and the characteristics of the AEM are derived therefrom [88, 115].

Assuming that the chassis displacement is zero and the dynamics of the engine, Lee and Lee [65] proposed a theoretical model to describe the dynamic characteristics of AEMs, which is expressed by the secondary path transfer function between the control voltage and the chassis, and the transmitted force in terms of the engine excitation force and the actuator motion. The theoretical model is verified by experiments, and the analytical results based on the proposed theoretical model agree well with the experimental results and confirm that the proposed theoretical model accurately describes the dynamic behaviour of an AEM. Considering the dynamics of actuator, the dynamics of the fluid in the inertia track, the structural parameter of the AEM, and the chassis displacements, Lee and Lee [66] proposed a modified linear AEM model that is expressed by the transmitted force in terms of the engine excitation force and the chassis force and the secondary path transfer function between the active force of the actuator and the engine excitation force or chassis force. The modified linear AEM model is verified by an experimental apparatus for measurement of the dynamic characteristics of an ACM, which shows that the simulation results based on the proposed modified linear AEM model and the experimental test are in agreement with fair accuracy. Considering the dynamics of the actuator, the dynamics of the fluid in the inertia track, the structural parameter of the AEM, the chassis displacements, the frequency-dependent characteristics of the volumetric stiffness of the main liquid chamber, and the complex stiffness of the main rubber spring, Hausberg [103] proposed a theoretical model expressed in the Laplace domain to describe the dynamic characteristics of an AEM. The proposed theoretical model is expressed by the cross point and driving point dynamic stiffness of the AEM at the engine side and the secondary path transfer function between the control voltage and the chassis (engine). The simulated curves of theoretical model proposed by Hausberg are in good agreement with the experimental results.

3.2. Finite-Element Model. Olsson [116] studied a three-point suspended 5-cylinder combustion diesel engine, as shown in Figure 7, which is attached to the vehicle body on the LHS (left-hand side) and RHS (right-hand side) via two rubber engine mounts and connected to the subframe via a TR (torque rod) with rubber bushings at both ends. Then, a finite-element model was proposed by ADAMS. The engine and torque rod are modelled with 12 kinematical degrees of freedom (DOFs) using rigid body representation. The LHS engine mount, RHS engine mount, and rubber bushings are modelled using 6 DOFs. Finally, the body and subframe attachment points are regarded as rigid in all directions. The finite-element model was not compared with the theoretical model or experimental model by Olsson in this article.

3.3. Identification (Experimental Model). The identification of the AEM shown in Table 1 is significant in the verification of the theoretical model, the controller design, and the dynamic characteristics of the AEM. The primary path is the transfer path between the error sensor and the disturbance source. The transfer path between the error sensor and the controller output is named the secondary path. The identification of the primary path or the secondary path is required for model-based control. Identification techniques include harmonic identification [57, 66], LMS- or FBLMS-based finite impulse response (FIR) identification [69],

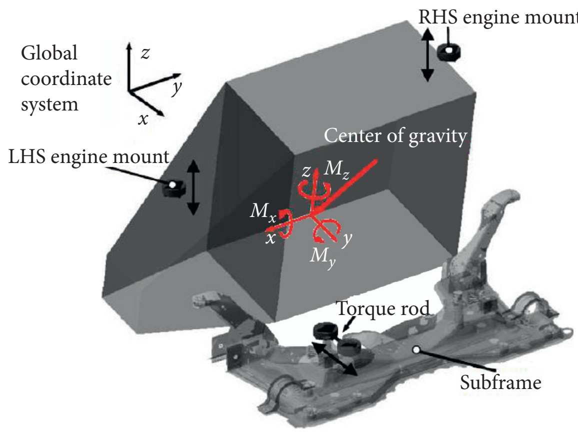

Figure 7: Engine model with engine suspension layout [116].

Table 1: Summary of AEM model and control.

Ref.	Year	Model	Controller	Model verification	Control verification
Riley et al. [117]	1995	Identification	FXLMS/AC	—	V
Nakaji et al. [57]	1999	FRT identification	SFX/AC	—	R/V
Aoki et al. [9]	1999	—	SFX/AC	—	V
Lee et al. [64]	2000	Theoretical model	Normalized FXLMS/AC	E	R
Fursdon et al. [51]	2000	—	Self-tuning cancellation/AC	—	V
Yang et al. [118]	2001	Theoretical model	FXLMS/AC&RC	E	S/R
Lee and Lee [65]	2002	Theoretical model	FXLMS	E	R
Togashi and Ichiryu [58]	2003	Theoretical model	FXLMS/AC	—	R
Kowalczyk et al. [1]	2004	FRT identification	FXLMS/AC and disturbance observer	—	V
Hillis et al. [52]	2005	Identification	Narrow-band FXLMS/AC	—	V
		—	Er-MCSI/AC	—	V
Hillis et al. [119]	2005	Theoretical model	Er-MCSI/AC	—	R/V
		Theoretical model	NBMCS/AC	—	R/V
Bouzid et al. [120]	2005	Identification	FXLMS/AC	—	S
		SI identification	H_∞/RC	E	S
Olsson [116]	2006	Finite-element model	Gain scheduled H_2/RC	—	Co-S
Shi Wenku and Chai [121]	2006	Theoretical model	FXLMS/AC	—	S
Karimi and Lohmann [122]	2007	Theoretical model	Haar wavelet-based H_∞/RC	—	C
Shin [123]	2007	—	OL&STAFC	—	S
Darsivan et al. [124]	2008	Theoretical model	EMRAN/IC	—	S
		—	PID/CC	—	S
		Identification	NARMA-L2 neural/IC	—	S
Lee &Lee [66]	2009	Theoretical model	Current shaping control	FRT identification	R
Darsivan et al. [125]	2009	Identification	NARMA-L2 neural network/IC	—	S
		—	PD.PID/CC	—	S
Fakhari et al. [126]	2010	Theoretical model	H_2 and H_∞/RC	—	S
Hillis [127]	2011	FBLMS identification	Narrow-band FXLMS/AC	—	V
Mahil et al. [128]	2011	Theoretical model	PID/CC	—	S
		Theoretical model	LQR/CC	—	S
Togashi et al. [59]	2011	—	Modified LMS/AC	—	S/V
		—	LMS/AC	—	S/V
Mansour et al. [71]	2012	Theoretical model	CL	—	R
Fok et al. [129]	2012	FRT identification	H_∞/RC	—	R
Fakhari and Ohadi [130]	2012	Theoretical model	H_2 and H_∞/RC	—	S

Table 1: Continued.

Ref.	Year	Model	Controller	Model verification	Control verification
Fakhari et al. [110]	2013	SI identification	Robust MRAC	—	S
		SI identification	H_∞/RC	—	S
Raoofy et al. [131]	2013	Theoretical model FIR filters identification	Narrow-band FXLMS/AC	—	S
Sun et al. [132]	2013	Theoretical model	LMI-based H∞/RC	—	S
Mahil et al. [133]	2014	Theoretical model	PID/CC	—	S
		Theoretical model	LQR/CC	—	S
Hausberg et al. [134]	2014	—	Newton/FXLMS with parameter-map/AC; Newton/FXLMS with parallel-map/AC	—	V
Fakhari et al. [135]	2015	Theoretical model	Robust MRAC	FRT identification	R
Vahdati and Heidari [69]	2015	Theoretical model	FXLMS/AC	LMS identification	S
Hausberg et al. [85]	2015	Theoretical model	Narrow-band FXLMS/AC	E	—
Hausberg et al. [3]	2016	FRT identification	Newton/FXLMS extended with grid-based look-up tables/AC	—	S/V
Guo Rong et al. [136]	2017	Theoretical model	PSO optimize the PID	—	S/V
Guo Rong et al. [137]	2017	Theoretical model	Extended FXLMS/AC	FRT identification	S

C/S/R/V: calculation/simulation/rig test/vehicle test; E: experimental identification; CL: closed loop; OL: open loop; CC: classical control; STAFC: single-tone adaptive feedforward control; AC: adaptive control; RC: robust control; IC: intelligent control; FXLMS: filtered-x least mean square; SFX: synchronized filtered-x least mean square; LMS: least mean square; Er-MCSI: error-driven minimal controller synthesis; NBMCS: narrow-band minimal controller synthesis; FBLMS: fast-block least mean square; NARMA: nonlinear autoregressive moving average; --: not discussed by author; FRT: frequency response techniques; SI: subspace identification; PSO: particle swarm optimization; MRAC: model reference adaptive control.

subspace identification [120], and neural network identification [138], all of which have been implemented in the identification of AEMs.

3.3.1. Frequency Response Measurements. Scholars have estimated AEM models by harmonic identification [129, 139]. For the identification of the actuator dynamics, the harmonic identification tests shown in Figure 8 were applied using a commercial rubber testing machine by Lee et al. [100].

Fakhari et al. [135] carried out the identification test shown in Figure 9(a), which identified the transfer function of the passive parts between the control force of the electromagnetic actuator and the output displacement of the AEM on the engine side. As shown in Figure 9(b), the transfer function of the active parts between the control force and the input current of the electromagnetic actuator is identified. Then, the secondary path transfer function of the AEM is proposed through the transfer function of the passive part times the transfer function of the active part.

Yang et al. [118] carried out a test to analyse the transfer properties of the AEM between the input current and the output force. Then, the approximate transfer function of the AEM was proposed by solving a nonlinear curve fitting problem.

3.3.2. LMS and FBLMS Identification. A finite impulse response (FIR) filter can be modelled as the estimate of the secondary path. Modelling errors between the secondary path and its estimate may lead to instability or serious performance degradation. The control system may be unstable when the phase error between the secondary path and its estimate is not less than 90° [140]. Broadband white noise can be used as an input signal in dynamical models, and the transfer function of the secondary path can be identified by the LMS identification algorithm. As shown in Figure 10, an LMS filter can identify the secondary path.

However, the LMS identification algorithm cannot cancel interference from the input engine vibration, which can be resolved by a fast-block LMS (FBLMS) in the frequency domain. FBLMS identification is robust to large system parameter variations, unknown or unmodelled dynamics, and nonlinear effects. Shynk [142] explained the general structure of FBLMS. As shown in Figure 11, the FBLMS identification algorithm is applied to a MIMO AEM system. The MIMO FBLMS filter updates the equation of the K^{th} length L data block [127], which is expressed as

$$\begin{cases} \hat{s}_{11}(K+1) = v\hat{s}_{11}(K) + \mathcal{F}^{-1}\left[u_1(z_k)B_1^*(z_k)F(z_k)\right]_{1:L}, \\ \hat{s}_{21}(K+1) = v\hat{s}_{21}(K) + \mathcal{F}^{-1}\left[u_2(z_k)B_1^*(z_k)F_2(z_k)\right]_{1:L}, \\ \hat{s}_{12}(K+1) = v\hat{s}_{12}(K) + \mathcal{F}^{-1}\left[u_1(z_k)B_2^*(z_k)F(z_k)\right]_{1:L}, \\ \hat{s}_{22}(K+1) = v\hat{s}_{22}(K) + \mathcal{F}^{-1}\left[u_2(z_k)B_2^*(z_k)F_2(z_k)\right]_{1:L}, \end{cases} \tag{9}$$

where $B_1(z_k)$ and $B_2(z_k)$ can be expressed by

$$\begin{cases} \operatorname{diag}\left[B_1(z_k)\right] = \mathscr{F}^{-1}\begin{bmatrix} b_1(K-1) \\ b_1(K) \end{bmatrix}, \\ \operatorname{iag}\left[B_2(z_k)\right] = \mathscr{F}^{-1}\begin{bmatrix} b_2(K-1) \\ b_2(K) \end{bmatrix}, \end{cases} \tag{10}$$

$$\begin{cases} F_1(z_k) = \mathscr{F}^{-1}\begin{bmatrix} 0_{L\times 1} \\ -e_1(K) - f_{11} - f_{12} \end{bmatrix}, \\ F_2(z_k) = \mathscr{F}^{-1}\begin{bmatrix} 0_{L\times 1} \\ -e_2(K) - f_{22} - f_{21} \end{bmatrix}, \end{cases} \tag{11}$$

where

$$\begin{cases} f_{11} = \mathscr{F}^{-1}\left\{B_1(z_k)\mathscr{F}\begin{bmatrix} \widehat{s}_{11}(K) \\ 0_{L\times 1} \end{bmatrix}\right\}_{L+1:2L}, \\ f_{12} = \mathscr{F}^{-1}\left\{B_2(z_k)\mathscr{F}\begin{bmatrix} \widehat{s}_{12}(K) \\ 0_{L\times 1} \end{bmatrix}\right\}_{L+1:2L}, \\ f_{22} = \mathscr{F}^{-1}\left\{B_2(z_k)\mathscr{F}\begin{bmatrix} \widehat{s}_{22}(K) \\ 0_{L\times 1} \end{bmatrix}\right\}_{L+1:2L}, \\ f_{21} = \mathscr{F}^{-1}\left\{B_1(z_k)\mathscr{F}\begin{bmatrix} \widehat{s}_{21}(K) \\ 0_{L\times 1} \end{bmatrix}\right\}_{L+1:2L}, \end{cases} \tag{12}$$

where $\mathscr{F}$ represents the fast Fourier transform (FFT).

3.3.3. Other Identification. Subspace identification [143, 144] was carried out to achieve the frequency responses from the input to the output of the system, as shown in Figure 12(a). The transfer functions G_{dyd} represent the frequency response between the disturbance and the response. In general, G_{io} represents the transfer function from the input i to the output o. The transfer function between the secondary source (the input u) and the error signal (the output y_u) and the transfer function between the disturbance signal and the error signal were identified by Seba et al. [120].

The neural network identification shown in Figure 12(b) can be defined mathematically for the NARMA-L2 neural network controller as the following equation:

$$\begin{aligned} \widehat{y}(k+d) = {} & f\left[y(k), y(k-1), \ldots, y(k-n+1),\right. \\ & \left. u(k-1), \ldots, u(k-m+1)\right] + g\left[y(k),\right. \\ & y(k-1), \ldots, y(k-n+1), u(k-1), \ldots, \\ & \left. u(k-m+1)\right] \cdot u(k), \end{aligned} \tag{13}$$

where $u(k)$ is the system input, $y(k)$ is the system output, and d is the delay of the parameters. The NARMA-L2 neural network controller identifies the inverse of the control plant. The control input to the plant can be determined by the equation expressed as

$$u(k) = \frac{y_r(k+d) - f\left[y(k), y(k-1), \ldots, y(k-n+1), u(k-1), \ldots, u(k-m+1)\right]}{g\left[y(k), y(k-1), \ldots, y(k-n+1), u(k-1), \ldots, u(k-m+1)\right]}. \tag{14}$$

4. Control Strategies

To improve the vibration control performance of AEM, many investigators have implemented various control algorithms, such as PID [50], adaptive control [121], robust control [132], and 2DOF control. Table 1 shows a summary of the control strategies applied during the last 2 decades, which are discussed in the following section.

4.1. Classical Control. PID control applied in AEMs continuously calculates an error value between a desired set point and the measured variable [124, 125, 128, 145]. The PID controller is mainly applied in the control of single-input-single-output (SISO) systems. It is difficult to control MIMO systems with the PID controller based on the transfer function.

The linear quadratic regulator (LQR) can overcome the aforementioned drawbacks of PID [126, 128, 146]. The weights of Q and R are adjusted, and the value of the gain K is calculated. The optimal results are obtained when R and Q are determined by various iterations. With $Q = \operatorname{diag}(10^9, 10^9, 10^9, 10^9)$, the LQR controller R was set to be unity by Mahil et al. [128] to obtain a better AEM performance. Classical control has been assessed but found to be deficient.

4.2. Adaptive Control. To tackle the high uncertainty of complex and variable environments, modern adaptive control is increasingly being applied. The AEM system is a time-varying system, which requires adaptive control. This control method can attenuate the vibration by adjusting the frequency and amplitude of the AEM actuator.

4.2.1. LMS. In 1960, a highly simplified recursive algorithm was developed by Widrow and Hoff [147] to calculate the optimal filter, named the LMS algorithm. To simplify the control strategies, as shown in Figure 13, the LMS algorithm can be verified by setting G to 1 and by setting error signal as the input signal for controlling the AEM.

The error signal $e[n]$ and the weight vector w_i of the modified LMS algorithm are expressed by

$$\begin{aligned} e[n] &= d[n] - y[n] = d[n] - \sum_{i=1}^{N} w_i e[n-i], \\ w_i[n+1] &= w_i[n] + 2\mu e[n] e[n-i], \quad i = 1, 2 \ldots N. \end{aligned} \tag{15}$$

Vehicle test results show that the transmitted force, seat rail vibration, and interior noise can be simultaneously attenuated by the modified LMS controller over a wide frequency band. The LMS controller only can reduce the amplitude at a certain frequency corresponding to a

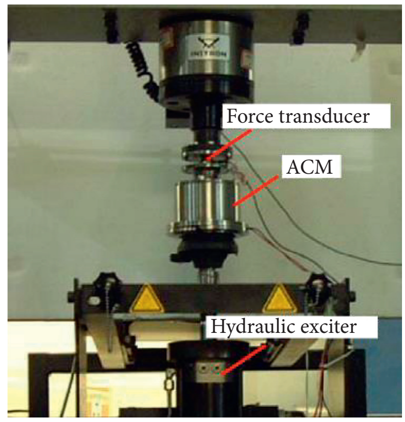

Figure 8: Harmonic identification tests [100].

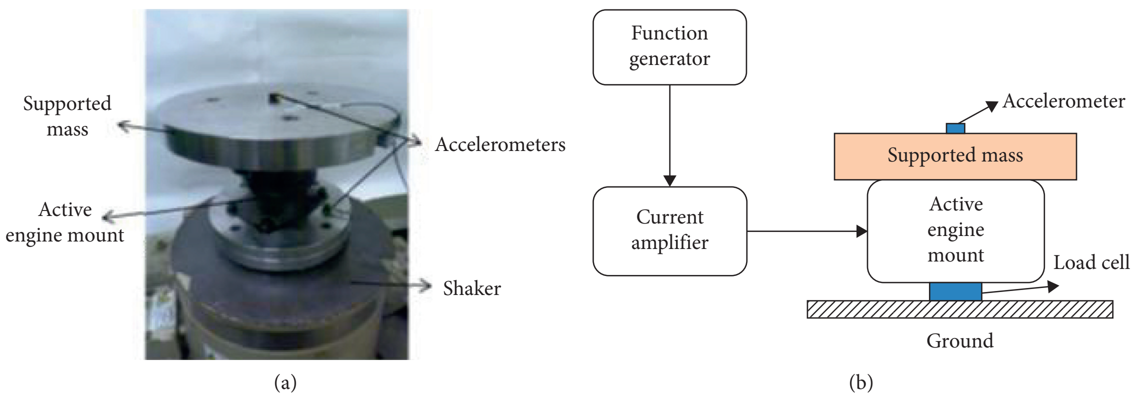

Figure 9: Identification of the AEM [135]: (a) passive component of AEM identification; (b) active component of AEM identification.

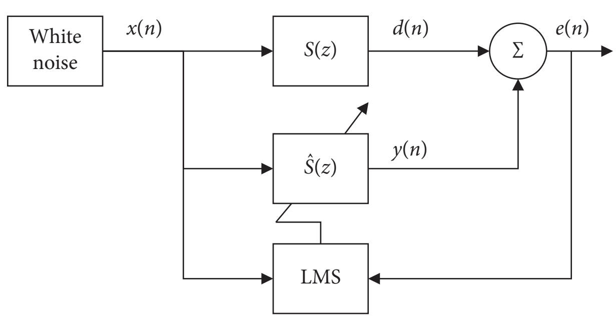

Figure 10: Identification of the secondary path using FIR filters [131, 141].

reference signal and cannot simultaneously attenuate the amplitude over a wide frequency band.

4.2.2. Filtered-X Least Mean Squares. Conover et al. [148, 149] proposed the filtered-x least mean squares (FXLMS) algorithm, which has been described in detail by other scholars [111–114]. The FXLMS control algorithm has become the primary tool to reduce active vibration or noise. As shown in Table 1, the FXLMS algorithm is the most common control strategy for controlling AEMs.

Figure 14 shows the block diagram of the normalized FXLMS algorithm for AEM control, which uses the engine RPM as the reference signal and the transmitted force from the engine to the chassis or body as the error signal for the generation of the actuator signal. The main design parameters of the FXLMS algorithm are the step size or the convergence coefficient, filter length, and leaky factor. The convergence speed of the FXLMS algorithm is influenced by the step size. When the filter converges to a steady state, the step size has a slight influence on the performance. The overall system stability is influenced by the leaky factor. The sampling rate and available computer specifications are influenced by the filter length. Table 2 shows that the sampling frequency, step size, filter length, and leaky factor vary in different studies. The FXLMS algorithm requires an

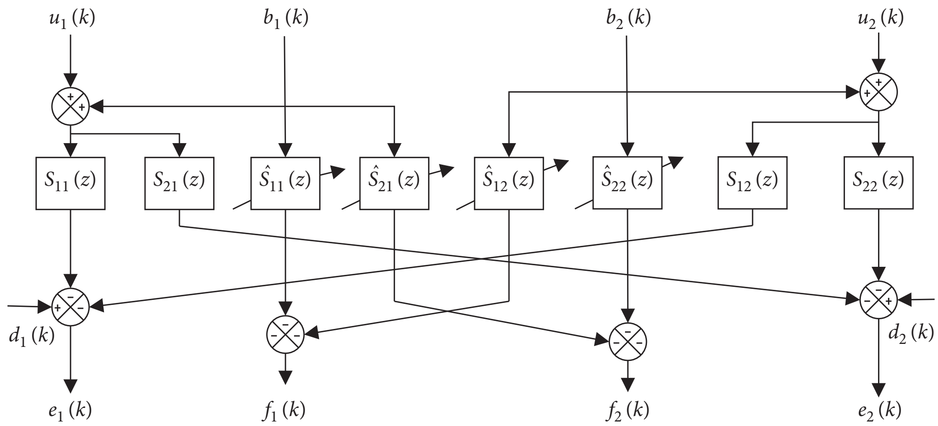

Figure 11: MIMO online system identification [127].

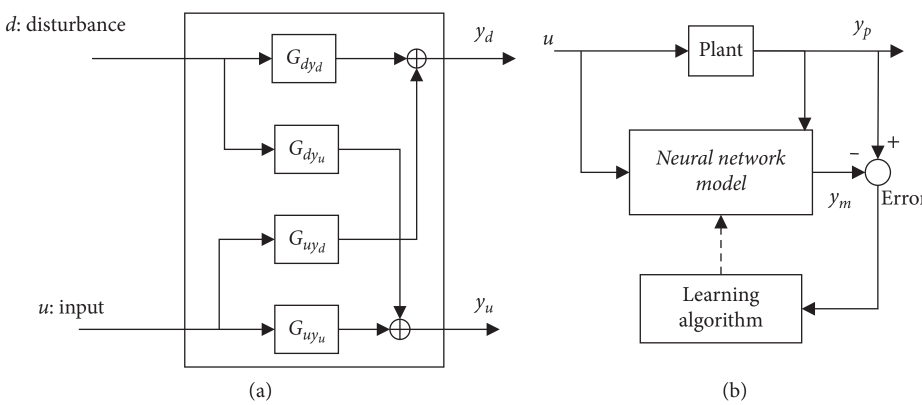

Figure 12: Block diagram of identification: (a) subspace identification [120]; (b) neural network identification [124, 125, 138].

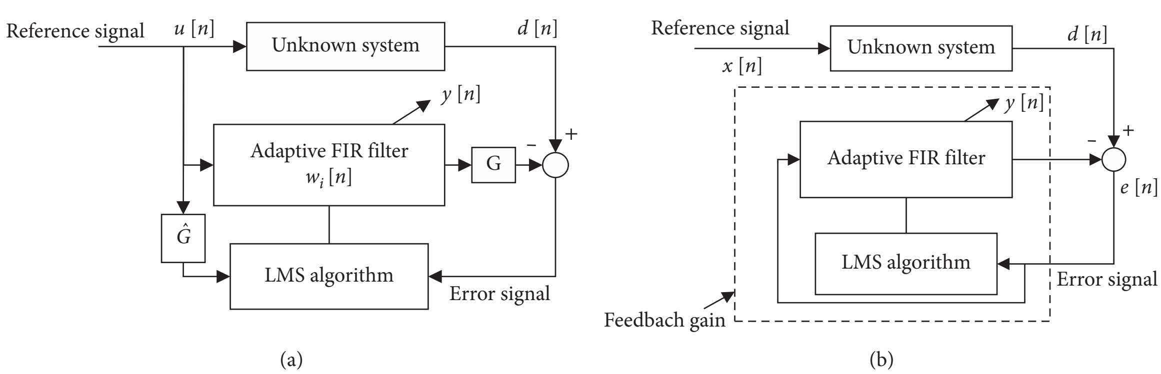

Figure 13: Block diagram of the LMS in the AEM [59]: (a) LMS; (b) modified LMS.

estimate of the secondary path of the AEM because model errors can cause performance degradation or instability of the FXLMS algorithm. To reduce the errors of model, an online system identification scheme is employed by Bao et al. [133]. In addition, the robustness of algorithm [150–152] must be improved to reduce the impact of errors on the control algorithm.

To control more than one AEM, Hillis [127] applied a MIMO narrow-band FXLMS algorithm to a system of two AEMs. The control equation is defined as

$$u[k] = w_1[k]x_1[k] + w_2[k]x_2[k]. \tag{16}$$

The reference signal is defined by

$$\begin{cases} x_1[k] = \sin(i\omega_e k\Delta), \\ x_2[k] = \cos(i\omega_e k\Delta), \end{cases} \tag{17}$$

where ω_e is the engine crankshaft rotation frequency, i is the engine order, and Δ is the sampling interval.

The weight vectors $\{w_1(k) \in \Re^{q\times 1}, w_2(k) \in \Re^{q\times 1}\}$ are updated according to

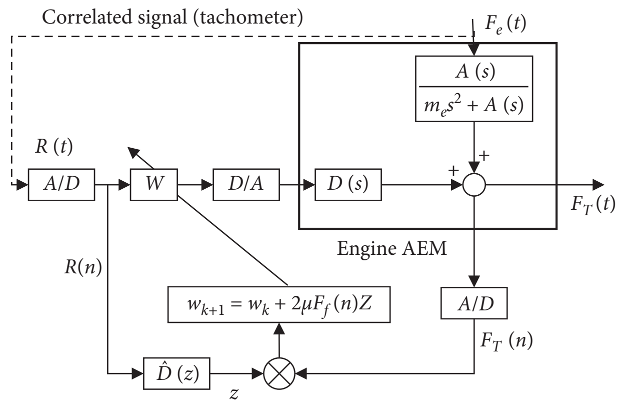

Figure 14: Diagram of normalized FXLMS [65].

Table 2: Parameters in the FXLMS algorithm.

Ref.	Year	Sampling frequency	Step size	Filter length	Leaky factor
LEE et al. [64]	2000	4 kHz	Conservatively small	150	—
Hillis et al. [52]	2005	4 kHz	—	32	—
Bouzid et al. [120]	2005	2 kHz	Normalized 0–2	—	0.9995
Hillis [127]	2011	4 kHz	—	128	—
Raoofy et al. [131]	2013	2 kHz	10^{-6}	10	—
		2 kHz	10^{-7}	10	—
Vahdati and Heidari [69]	2015	5 KHz	0.0002	120	—
Guo Rong et al. [137]	2017	—	10^{-6}	50	—

$$\begin{cases} w_1[k+1] = \nu w_1[k] - 2\mu x_1'(k)e(k), \\ w_2[k+1] = \nu w_2[k] - 2\mu x_2'(k)e(k), \end{cases} \tag{18}$$

where μ and ν are the step size and leakage factor, respectively. To avoid the accumulation of numerical rounding errors, the leakage factor is applied to the tap weights. $\{x_1'(k), x_1'(k)\} \in \mathfrak{R}^{q\times p}$ are the filtered matrices of the reference signals $\{x_1, x_2\}$, which can be expressed by

$$\begin{cases} x_1'(k) = \widehat{S}^T(z)x_1[k], \\ x_2'(k) = \widehat{S}^T(z)x_2[k], \end{cases} \tag{19}$$

where $\widehat{S}^T(k) \in \mathfrak{R}^{p\times q}$ is the matrix of the estimation of the secondary path transfer function, which is described by

$$\widehat{S}(k) = \begin{bmatrix} \widehat{S}_{11} & \widehat{S}_{12} & \cdots & \widehat{S}_{1q} \\ \widehat{S}_{21} & \widehat{S}_{22} & \cdots & \widehat{S}_{2q} \\ \vdots & \vdots & \ddots & \vdots \\ \widehat{S}_{p1} & \widehat{S}_{p2} & \cdots & \widehat{S}_{pq} \end{bmatrix}. \tag{20}$$

The proposed MIMO FXLMS algorithm was applied to a two-mount/two-sensor system fitted to a saloon car equipped with a four-cylinder two-litre turbo-diesel engine. Vehicle tests indicate that the controller typically reduces chassis vibration by 50 percent to 90 percent under normal driving conditions.

Synchronized filtered-x least mean square (SFX) is a modified form of the FXLMS algorithm with a limited application to cyclic phenomena [56, 57]. Under this application environment, SFX has a computational advantage compared with the FXLMS algorithm. SFX has the ability to control higher order components and straight convergence. The control output of SFX is expressed as

$$y(n) = \sum_{i=0}^{I-1} w_n(i) \sum_{a=-\infty}^{\infty} \delta(n - aI - i). \tag{21}$$

The filter weights and reference signal are, respectively, expressed by

$$\begin{gathered} w_i(n+1) = w_i(n) - \mu e(n) r(n-i), \\ r(n) = \sum_j \widehat{c}_j x(n-j). \end{gathered} \tag{22}$$

Vehicle tests show that reductions in the vehicle idle vibration, the boom noise during driving, and the higher order boom noise during idling are achieved by the proposed SFX controller [56].

Lee et al. [3, 134, 153] proposed the Newton FXLMS algorithm, the filter weight of which is expressed by

$$w(n+1) = w(n) - \mu\widehat{S}^{-1}(r\omega)e^{-jr\omega nT}e(n). \tag{23}$$

Simulations show that the Newton FXLMS control has an equal convergence rate at different engine speeds, while the FXLMS control has different convergence rate at different engine speeds. To tackle the limited convergence time and the tracking speed, as shown in Figure 15, online adapted look-up tables were incorporated as parameter-maps or parallel-maps, respectively, into the proposed Newton FXLMS algorithm. The look-up tables store the initial conditions of the Newton FXLMS, which is the filter weight vector $w(0)$ that is passed from the look-up tables to

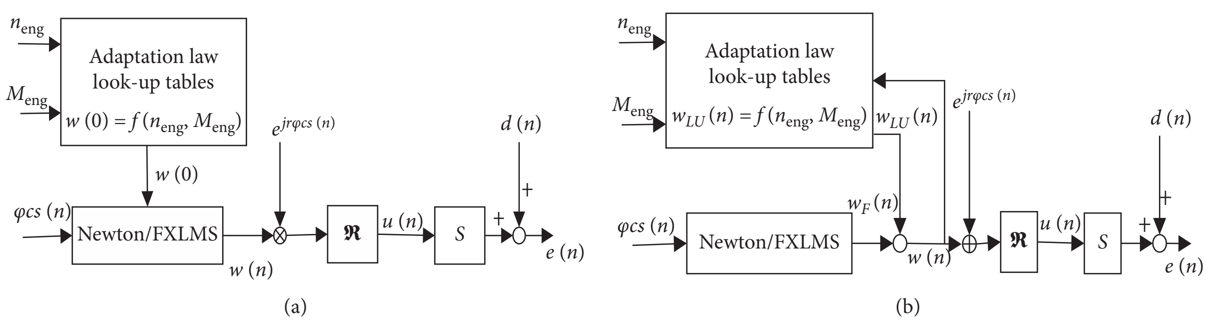

FIGURE 15: Newton FXLMS with look-up tables [3, 134, 153]: (a) Newton FXLMS with parameter-map; (b) Newton FXLMS with parallel-map.

the Newton FXLMS before activating the Newton FXLMS with the parameter-map. The look-up table is applied in parallel to the Newton FXLMS, which is the Newton FXLMS with the parallel-map. The output w_{LU} of the parallel-map can be expressed as

$$w_{LU} = \sum_{k=1}^{K}\sum_{l=1}^{L} \theta_{k,l}\Phi_{k,l}(y,c). \quad (24)$$

The vector of the table data is adapted online with the algorithm, which is expressed by

$$v_i(n+1) = v_i(n) + \mu_{LU}\frac{e_{LU}(n)\Phi_i(y(n),c)}{\sum_{j=1}^{K.L}\Phi_j^2(y(n),c)}, \quad i = 1,2,\ldots,K.L. \quad (25)$$

The step size μ_{LU} is different from the step size μ of the FXLMS. μ is set to 0.001 and μ_{LU}<0.0005, which will suppress short-term variations of the training signal.

Vehicle tests show that the proposed control strategy applied on the AEM can reduce the convergence time. When μ is set to 0.001, the Newton FXLMS with the parameter-map or the parallel-map completely attenuates the vibration with almost no convergence time. The tracking behaviour is improved by the Newton FXLMS algorithm with the parallel-map control applied on the AEM, while the tracking performance remains unchanged for the Newton FXLMS algorithm with the parameter-map.

As shown in Figure 16, body input point inertance (IPI) and extended FXLMS were proposed by Guo et al. [137]. The transmitted force to the chassis is converted to an acceleration, which is set to the error signal. The IPI is expressed as

$$\mathrm{H}_{a/F}(\omega) = \frac{\ddot{X}}{F}, \quad (26)$$

where $\ddot{X}$, F, and ω are the acceleration, transmitted force to the chassis, and angular frequency of the engine crankshaft angle, respectively. The weight coefficient can be expressed as

$$W(n+1) = (1-\alpha\mu)W(n) - 2\mu e(n)R(n), \quad (27)$$

where α is the leakage coefficient, μ is the step size, and $R'(n)$ is the "filtered" reference signal vector.

Compared with the uncontrolled AEM, the simulation results show that the acceleration on the AEM has decreased by 80 percent for most of the time domain after applying the extended FXLMS controller.

4.2.3. Minimal Controller Synthesis (MCS). The minimal control synthesis (MCS) requires no knowledge of the parameters and achieves stability and robustness [154]. The Er-MCSI controller shown in Figure 17 is a derivation of the MCS controller. The control law of the Er-MCSI is expressed as

$$u(n) = K_e(n)x_e(n) + K_I(n)x_I(n), \quad (28)$$

where $x_e(n)$ is the state error and x_I is the scalar discrete-time integral of the output error signal. The update law of the controller gains can be expressed as

$$\begin{cases} K_e(t) = K_e(n-1) + \beta q_e(n) - \sigma q_e(n-1), \\ K_c(t) = K_I(n-1) + \beta q_I(n) - \sigma q_I(n-1), \end{cases} \quad (29)$$

where

$$\begin{cases} q_e = y_e x_e^T, \\ q_I = y_e X_I, \\ \sigma = \beta - \alpha\Delta, \end{cases} \quad (30)$$

where α and β are weights and y_e and Δ are the output error and the sampling interval, respectively.

The proposed Er-MCS controller was applied on an AEM, which is fitted to a car equipped with a four-cylinder engine. Test results show that the Er-MCS algorithm performed similarly to the FXLMS algorithm in terms of the cancellation level and convergence speed, and the Er-MCS algorithm has a significant computational advantage compared with the FXLMS algorithm. When the Er-MCSI is applied to control multiple AEMs and multiple sensor systems, the computational advantage will become more significant.

To tackle narrow-band error signals or the narrow-band component of broadband signals, the narrow-band MCS (NBMCS) controller shown in Figure 18 was developed based on the Er-MCSI by Hillis et al. [119]. For the MCS algorithm, the plant parameters are unknown or

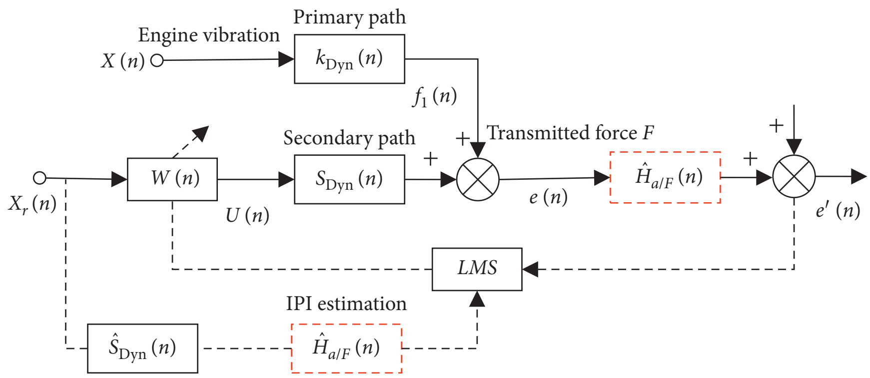

Figure 16: Extended FXLMS algorithm [137].

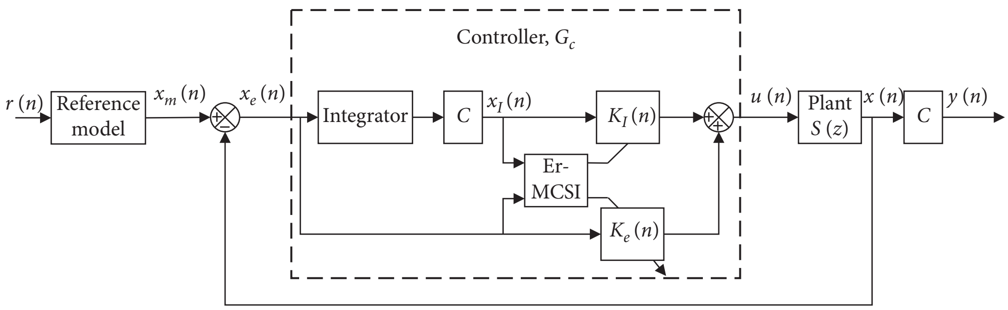

Figure 17: Er-MCSI controller [52].

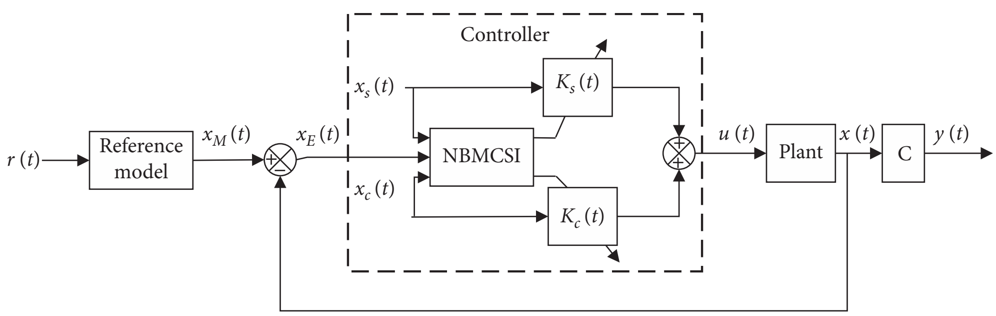

Figure 18: Block diagram of the NBMCS controller [119].

time-varying. For the NBMCS, the disturbance frequency must be known or measured.

The control equation is defined as

$$u(t) = K_s(t)x_s(t) + K_c(t)x_c(t), \tag{31}$$

where $x_s(t)$ and $x_c(t)$ are described by

$$\begin{cases} x_s(t) = \sin(\omega t), \\ x_c(t) = \cos(\omega t). \end{cases} \tag{32}$$

The proposed NBMCS algorithm was compared with the Er-MCSI algorithm using simulations and implementation with an AEM fitted to a diesel engine saloon car [119]. When the frequency of the disturbance is known or measured, the simulations and vehicle tests show that the NBMCS algorithm outperforms the broadband Er-MCSI algorithm in narrow-band applications and overcomes the gain windup problem in the Er-MCSI.

4.3. Robust Control. Accurate models of the AEM system are difficult in model-based control, and controllers may not achieve the desired performance due to model uncertainties, disturbances, and noise. Robust controllers have robust performance in the presence of perturbations, such as disturbance, noise, parametric uncertainties, and unmodelled dynamics [155, 156].

To attenuate transmitted forces over a large frequency band from the engine to the chassis, the gain scheduled H_2 controllers applied on an AEM by Olsson [116] can work well with system nonlinearities and engine vibration, but they do not work well at extremely high ramping speeds and nominal engine torque.

To isolate the engine vibration and prevent actuator saturation in the case of perturbations, Fakhari et al. [110, 126, 130] applied the H_2 and H_∞ controllers shown in Figure 19. The weighting functions W_n, $[W_d]_{6\times6}$, W_F, and W_u are the sensor noise, disturbances, transmitted force, and

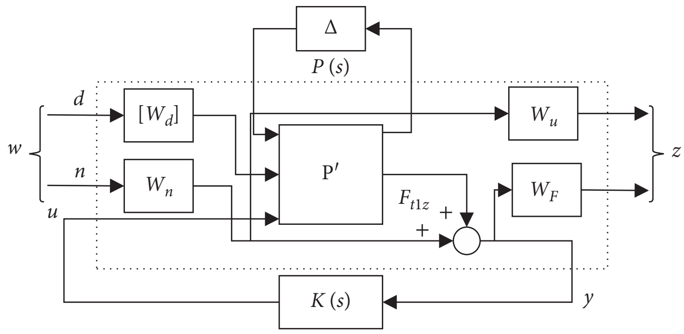

Figure 19: The closed-loop system [110].

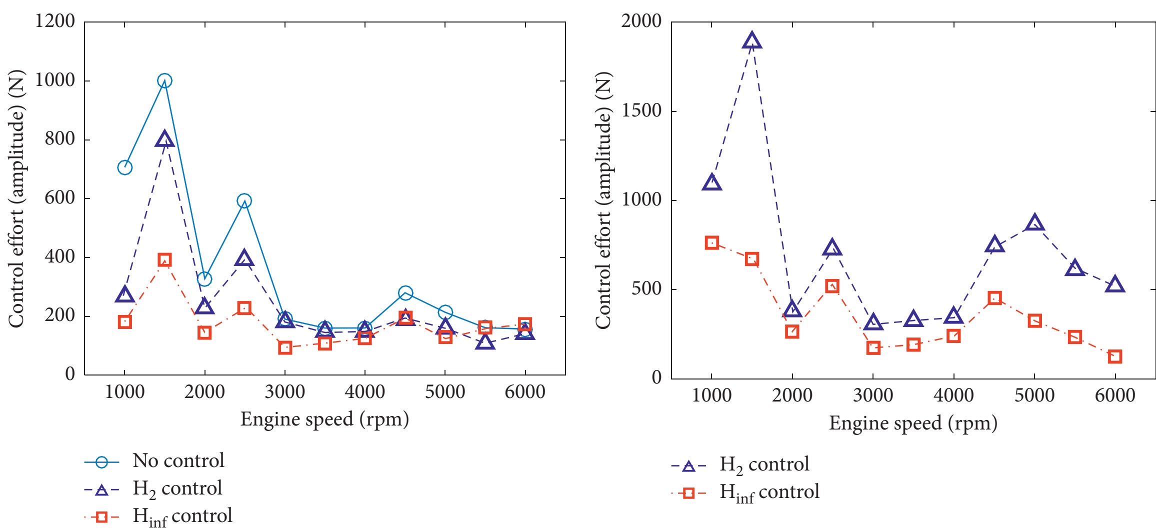

(a) (b)

Figure 20: Control performances [130].

input current to the actuator, respectively. μ-analysis was used to evaluate the robust stability of the controllers. Using the Hankel-norm approximation method, the order of the H_2 and H_∞ controllers can be set to 16 and 14, respectively, for low cost, easy commissioning, high reliability, and the maintenance of the controller.

Simulations were carried out by Fakhari and Ohadi [130] to evaluate the effectiveness of an AEM in vibration suppression of a four-cylinder engine using the closed-loop system with H_2 and H_∞. Compared with the H_∞ control, the simulation shown in Figure 20 indicates that the H_2 control requires a greater control effect to achieve the control performances. Meanwhile, robust performance and stability of the closed-loop system are achieved with H_2 and H_∞.

4.4. 2DOF Control. To solve the disadvantage of nonadaptive control and adaptive control, researchers have studied 2DOF controllers, such as integrating open- and closed-loop control methods for AEMs [157]. In the case of perturbations, such as disturbance, noise, and unmodelled dynamics, the conventional adaptive control system may become unstable, while the robust approaches are still robust [155, 156]. When there are nonparametric uncertainties, the robust adaptive strategy can conquer the behaviour of the adaptive controller. The robust adaptive controller can overcome the conservative behaviour of the robust controller.

By selecting a proper reference model, the robust model reference adaptive control (MRAC) method based on the modified gradient method was proposed by Ioannou et al. [135] and can be expressed as

$$u_p = \vec{\theta}^T \vec{\omega}, \tag{33}$$

where $\vec{\theta}$ is the controller parameters and $\vec{\omega} = [\vec{\omega}_1^T\ \vec{\omega}_2^T\ y_p\ r]$ is the state variables of the controller. The adaptive law can be expressed as

$$\begin{aligned} \dot{\vec{\theta}} &= -[\Gamma]\varepsilon\vec{\phi}\,\mathrm{sgn}(\rho^*), \\ \dot{\rho} &= \gamma\varepsilon\xi, \end{aligned} \tag{34}$$

where $\gamma > 0$. $[\Gamma] = [\Gamma]^T > 0$. $[\Gamma]$ and γ denote the adaptive gains. sgn and ρ are the sign function and the estimate of ρ^*, respectively. ρ^* can be expressed as $\rho^* = k_p/k_m$.

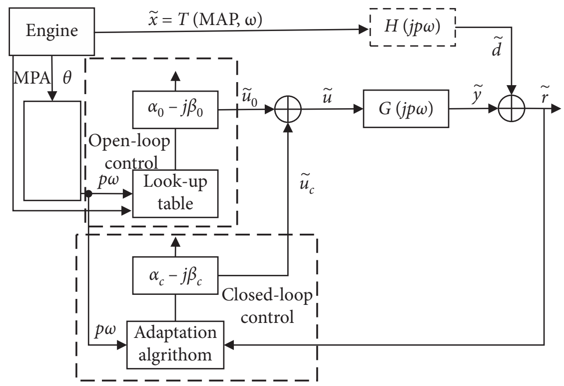

Figure 21: Frequency domain of the 2DOF control system [123].

An experimental setup was carried out by Ioannou et al. [135] to evaluate the vibration performance of an AEM with the proposed robust MRAC. Tests show that the proposed robust MRAC provides a better control performance than the P control with a phase shift in the case of large uncertainties. However, in the case of no uncertainties, the P control with a phase shift provides a better control performance than the proposed robust MRAC in a certain high frequency range.

To control the vibrations of the engine-chassis system, Yang [118] proposed a 2DOF control strategy applied on an AEM, which is formed of an H_∞ robust feedback controller and a FXLMS feedforward controller. The weight is represented as

$$W(n+1) = \mathrm{W}(n) + \mu E(n) X_{\hat{c}}(n), \quad (35)$$

where $X_{\hat{c}}(n)$ is the filtered input and $E(n)$ is the error. The robust feedback controller is designed by μ-synthesis. To achieve control through a personal computer, the order of the robust controller was reduced from 23 to 7, which attenuated the vibration from the engine to the chassis, and robustness was achieved.

As shown in Figure 21, open-loop control is designed based on the manifold absolute pressure and crank speed. Based on the single-tone adaptive feedforward control, closed-loop control is designed. The update algorithm in discrete-time implementation is expressed as

$$\tilde{u}_{c,\text{new}} = \tilde{u}_{c,\text{old}} - \gamma \tilde{G}^* (jp\omega) Q \tilde{r}_{c,\text{old}}. \quad (36)$$

Simulations show that fast response times and robustness to vehicle variations can be achieved at the same time by integrating open-loop and closed-loop controls.

5. Conclusions

Based on the above review, the difficulties and trends in the research of modelling and controlling AEMs are summarized as follows:

(1) Most theoretical models are based on assumptions that are not always consistent with the working conditions of AEMs. The relative displacements (actuator, engine attachment point, and chassis attachment point), the frequency-dependent and amplitude-dependent characteristics of the elastomeric stiffness, and the damping should be considered. Similarly, theoretical models are oversimplified and do not consider complex interactions between the preload and the mass of the chassis, which can yield a vibration solution for one AEM fitted to different vehicles equipped with different engines.

(2) The method of AEM identification should be proposed to verify the above complex theoretical models and finite-element models of AEMs. Meanwhile, the effects of the AEM parameters (structural parameters and performance parameters) on the AEM dynamics should be carried out to design, manufacture, and control AEMs.

(3) The proposed closed-loop control system of AEM must be stable or robust in the case of high uncertainty in complex and variable environments, such as disturbance, noise, and unmodelled dynamics. The implementation of some controllers is sometimes costly and time-consuming. Thus, the demand of AEM control is the development and application of more advanced control approaches based on the principles of stability, robustness, intelligence, and optimality.

(4) The goal of the next generation of electromagnetic AEMs will be a compromise among a small volume, light weight, large actuator force, low cost, intelligence, and effectiveness under all working conditions.

Conflicts of Interest

The authors declare no potential conflicts of interest with respect to the research, authorship, and/or publication of this article.

Acknowledgments

The authors are grateful for the assistance of staff of NVH in the State Key Laboratory of Automotive Simulation and

Control, China. This work was financially supported by "863" National High Technology Research and Development Program (2007220101002381) and National Key R&D Program of China (Grant no. 2018YFB0106203).

References

[1] K. Kowalczyk, F. Svaricek, C. Bohn et al., "An overview of recent automotive applications of active vibration control," in *Proceedings of the RTO AVT–110 Symposium Habitability of Combat and Transport Vehicles: Noise Vibration and Motion*, IEEE, Prague, Czechia, October 2004.

[2] T. Inoue, A. Takahashi, H. Sano et al., "NV countermeasure Technology for a cylinder-on-demand engine-development of active booming noise control system Applying adaptive notch filter," in *Proceedings of the SAE Technical Paper*, IEEE, Detroit, MI, USA, March 2004.

[3] F. Hausberg, M. Plöchl, M. Rupp, P. Pfeffer, and S. Hecker, "Combination of map-based and adaptive feedforward control algorithms for active engine mounts," *Journal of Vibration and Control*, vol. 23, no. 19, pp. 3092–3107, 2016.

[4] D. Swanson, "Active engine mounts for vehicles," SAE, Warrendale, PA, USA, Technical Paper 932432, 1993.

[5] S. Römling, S. Vollmann, and T. Kolkhorst, "Active engine mount system in the new Audi S8," *MTZ Worldwide*, vol. 74, no. 1, pp. 34–38, 2013.

[6] A. Gennesseaux, "Research for new vibration isolation techniques: from hydro-mounts to active mounts," SAE, Warrendale, PA, USA, Technical Paper 931324, 1993.

[7] A. Renault, "Modelling of pneumatic engine mount," Master's Thesis, Chalmers University of Technology, Gothenburg, Sweden, 2005.

[8] A. Turnip, K.-S. Hong, and S. Park, "Modeling of a hydraulic engine mount for active pneumatic engine vibration control using the extended kalman filter," *Journal of Mechanical Science and Technology*, vol. 23, no. 1, pp. 229–236, 2009.

[9] A. Turnip and G. G. Redhyka, "Sensorless control with kalman filter in an active engine mount system," in *Proceedings of the International Conference on Intelligent Systems*, IEEE, Kuala Lumpur, Malaysia, February 2015.

[10] A. Turnip, L. H. Nguyen, S. Park et al., "Development of feed forward control algorithm for active pneumatic engine mount system," in *Proceedings of the KSME Dynamics and Control Division Spring Conference*, pp. 210–214, Berlin, Germany, May 2008.

[11] I. J. Kim, J. C. Lee, J. Y. Kim et al., "Identification of optimal control parameters for a pneumatic active engine mount system," *Transactions of KSAE*, vol. 20, no. 2, pp. 30–37, 2012.

[12] H.-W. Park, J.-C. Lee, J.-Y. Choi, and J.-H. Kim, "Correlation analysis of TPA output variables in a pneumatic active engine mount system," *Transactions of the Korean Society of Automotive Engineers*, vol. 20, no. 1, pp. 46–52, 2012.

[13] H. Ozaki, T. Tsukamoto, A. Ichikawa et al., "Development of active engine mount," in *Proceedings of the JSAE Annual Congress*, pp. 141–144, 1999.

[14] H. K. Bae, J. C. Lee, J. Y. Choi et al., "On the analysis of dynamic characteristics and parameter sensitivities of pneumatic active engine mount," in *Proceedings of the KSAE Department comprehensive academic conference*, Oxford University Press, Korea, pp. 547–551, May 2010.

[15] H. K. Bae, I. C. Yeo, J. C. Lee et al., "PILS (Processor-in-the-Loop simulator) of active pneumatic engine mount by dynamic neural network," in *Proceedings of the 2010 Korea Society Of Automotive Engineers Conference And Exhibition*, pp. 1091–1096, Oxford University Press, Korea, November 2010.

[16] H. W. Park, J. C. Lee, J. Y. Choi et al., "A computer simulation model and dynamic analysis of pneumatic active engine mount," in *Proceedings of the 2009 KSAE Department comprehensive academic conference*, pp. 533–538, ISSI, Korea, April 2009.

[17] I. C. Yeo, J. Y. Choi, W. H. Lee et al., "Experimental system identification of active pneumatic engine mount by dynamic neural network," in *Proceedings of the 2010 KSAE Department Comprehensive Academic Conference*, pp. 552–557, Oxford University Press.

[18] J. Y. Choi, N. S. Choi, and J. H. Kim, "Development and vehicle test on pneumatic type active engine mounting system," in *Proceedings of the 2011 Korea Society Of Automotive Engineers Partial Conference*, pp. 967–970, KSAE, korea, May 2011.

[19] H. W. Park, J. C. Lee, W. H. Lee et al., "Correlation in TPA output parameter of pneumatic active engine mount system," in *Proceedings of the 2009 Korean Society Of Automotive Engineers Conference And Exhibition*, pp. 1363–1366, KSAE, Korea, November 2009.

[20] I. J. Kim, J. C. Lee, and W. H. Lee, "The map of control performance for a pneumatic active engine mount using," in *Proceedings of the 2009 Korean Society Of Automotive Engineers Conference And Exhibition*, pp. 1339–1345, KSAE, Korea, November 2009.

[21] J. Y. Choi, W. H. Lee, J. H. Kim et al., "Development of pneumatic active engine mount," in *Proceedings of the Korean Society For Noise And Vibration Engineering Conference Autumn*, pp. 282-283, KSAE, Korea, November 2008.

[22] J. Y. Choi, W. H. Lee, H. C. Sohn et al., "An experimental study on control factor of pneumatic active engine mount," in *Proceedings of the KSNVE Conference 2009*, Korea Society For Noise And Vibration Engineering, pp. 450–451, Korea, April 2009.

[23] J. Y. Choi, J. H. Kim, and C. S. Kim, "A study on the performance of pneumatic type Active engine mounting system," in *Proceedings of the Korea Society For Noise And Vibration Engineering Conference 2011*, Korea Society For Noise And Vibration Engineering, Korea, pp. 512-513, April 2011.

[24] S. Chakrabarti and M. J. Dapino, "Coupled axisymmetric finite element model of a magneto-hydraulic actuator for active engine mounts," in *Proceedings of the Industrial and Commercial Applications of Smart Structures Technologies 2011*, IEEE, San Diego, CA, USA, March 2011.

[25] S. Chakrabarti and M. J. Dapino, "Design and modeling of a hydraulically amplified magnetostrictive actuator for automotive engine mounts," in *Proceedings of the Industrial and Commercial Applications of Smart Structures Technologies*, IEEE, San Diego, CA, USA, March 2010.

[26] V. Q. Nguyen and S. B. Choi, "A robust vibration control for a multi-active mount system subjected to broadband excitation," *Smart Materials and Structures*, vol. 20, no. 5, Article ID 055002, 2011.

[27] V.-Q. Nguyen, S.-M. Choi, S.-B. Choi, and S.-J. Moon, "Sliding mode control of a vibrating system using a hybrid active mount," *Proceedings of the Institution of Mechanical Engineers, Part C: Journal of Mechanical Engineering Science*, vol. 223, no. 6, pp. 1327–1337, 2009.

[28] W. K. Shi, H. T. Min, and Y. Qu, "Simulation analysis of vibration isolation for engine piezoelectric mount," *Piezoelectrics & Acoustooptics*, vol. 27, no. 5, pp. 560–586, 2005.

[29] W. K. Shi, R. Q. Zheng, and H. T. Min, "Simulation of vibration characteristics of active vontroled hydraulic mount with electrostrictive actuator," *Journal of System Simulation*, vol. 17, no. 10, pp. 2504–2507, 2005.

[30] W. K. Shi and R. Q. Zheng, "Simulation of vibration characteristics of active controlled hydraulic mount with electrostrictive actuator," *Journal of Jilin University (Engineering and Technology Edition*, vol. 35, no. 1, pp. 116–121, 2005.

[31] H. T. Min and W. K. Shi, "Piezoelectric mount and simulation analysis on active control for engine vibration," *Automotive Engineering*, vol. 26, no. 6, pp. 671–674, 2004.

[32] G. C. Sun, Y. T. Tian, and Y. Qu, "Adaptive control for automotive engine active vibration isolation system," *Automotive Engineering*, vol. 26, no. 1, pp. 38–41, 2004.

[33] H. Sui, "Finite element analysis of piezoelectric effect and research on piezoelectric suspension control method," Master's Thesis, Jilin University, Changchun, China, 2003.

[34] H. T. Min, "Study on dynamic characteristics simulation and active control theory of automobile powerplant mount system," Doctoral Thesis, Jilin University, Changchun, China, 2004.

[35] R. Kraus, M. Jonathan, H. Jan et al., "Experimental study on active noise and active vibration control for a passenger car using novel piezoelectric engine mounts and electro dynamic inertial mass actuators," in *Proceedings of the 25nd International Conference On Adaptive Structures And Technologies*, Hague, Netherlands, October 2014.

[36] S. Li, X. Xiong, and G. C. Shi, "Piezoelectric actuator design and application on active vibration control," *Physics Procedia*, vol. 25, pp. 1388–1396, 2012.

[37] S.-J. Moon, S.-M. Choi, V.-Q. Nguyen et al., "An inertia-type hybrid mount combining a rubber mount and a piezostack actuator for naval shipboard equipment," *International Journal of Naval Architecture and Ocean Engineering*, vol. 5, no. 1, pp. 62–80, 2013.

[38] F. Khameneifar, S. Arzanpour, and M. Moallem, "Piezo-actuated active decoupler hydraulic engine mount," in *Asme International Mechanical Engineering Congress & Exposition*, AMSE, Montreal, Canada, 2010.

[39] K. B. Scribner, L. A. Sievers, and A. H. von Flotow, "Active narrow-band vibration isolation of machinery noise from resonant substructures," *Journal of Sound and Vibration*, vol. 167, no. 1, pp. 17–40, 1993.

[40] D. Y. Lee, Y. K. Park, S. B. Choi et al., "Design and vibration control of vehicle engine mount activated by MR fluid and piezoelectric actuator," in *Proceedings of the Second International Conference On Smart Materials And Nanotechnology In Engineering*, Weihai, China, October 2009.

[41] S. B. Choi, J. W. Sohn, S. M. Choi et al., "A piezostack-based active mount for broadband frequency vibration control: experimental validation," *Smart Materials and Structures*, vol. 18, no. 9, Article ID 097001, 2009.

[42] H. Haldenwanger and P. Klose, "Isolation and compensation of vibration by means of active piezo-ceramic mounts," in *Proceedings Of the International Symposium On Advanced Vehicle Control*, JSAE, Yokohama, Japan, pp. 23–27, September 1992.

[43] T. Ushijima and S. Kumakawa, "Active engine mount with piezo-actuator for vibration control," SAE, Warrendale, PA, USA, Technical Paper 930201, 1993.

[44] T. Shibayama, K. Ito, T. Gami et al., "Active engine mount for a large amplitude of idling vibration," SAE, Warrendale, PA, USA, Technical Paper 951298, 1995.

[45] D. Mayer, S. Herold, W. Stücklschwaiger et al., "Realisation and test of an active engine mount system for automotive application," in *Proceedings Of the 5th International Styrian Noise*, Vibration & Harshness Congress, Graz, Austria, January 2008.

[46] R. Kraus, S. Herold, J. Millitzer et al., "Development of active engine mounts based on piezo actuators," *ATZ Worldwide*, vol. 116, no. 1, pp. 50–55, 2014.

[47] T. BEIN, S. HEROLD, and D. MAYER, "recent advances in active noise and vibration control," in *Proceedings of the 10th European Congress and Exposition on Noise Control Engineering*, Documenta, Maastricht, Netherlands, June 2015.

[48] M. Kauba, S. Herold, T. Koch et al., "Design and application of an active vibration control system for a marine engine mount," in *Proceedings of the International Conference on Isma Conference*, ISMA, Leuven, Belgium, September 2008.

[49] T. Bartel, H. Sven, M. Dirk et al., "Development and testing of active vibration control systems with piezoelectric actuators," in *Proceedings Of the 6th ECCOMAS Conference on Smart Structures and Materials*, Turin, Italy, June 2013.

[50] L. Mikael, K. Pasi, and N. K. Heikki, "Linear motion miniature actuators," in *Proceedings of the 2nd Tampere International Conference on Machine Automation*, Tampere University of Technology, Tampere, Finland, pp. 32–48, September 1998.

[51] P. M. T. Fursdon, A. J. L. Harrison, and D. P. Stoten, "The design and development of a self-tuning active engine mount," in *Proceedings of the ImechE European Conference on Vehicle Noise and Vibration*, Imeche, London, UK, May 2000.

[52] A. J. Hillis, A. J. L. Harrison, and D. P. Stoten, "A comparison of two adaptive algorithms for the control of active engine mounts," *Journal of Sound and Vibration*, vol. 28, pp. 637–654, 2005.

[53] P. M. T. Fursdon, *Active Vibration Control Method and Apparatus Applicable to a Vehicle Engine Mount*, UK PatentNo. GB2354054 (A), 2001.

[54] C. Hartwig, M. Haase, M. Hofmann et al., "Electromagnetic actuators for active engine vibration cancellation," in *Proceedings of the 7th International Conference on New Actuators ACTUATOR 2000*, EnglishView, Bremen, Germany, June 2000.

[55] H.-J. Karkosch, F. Svaricek, R. A. Shoureshi et al., "Automotive applications of active vibration control," in *Proceedings of the 1999 European Control Conference*, ISSN, Karlsruhe, Germany, September 1999.

[56] K. Aoki, T. Shikata, Y. Hyoudou et al., T. Shikata, Y. Hyoudou, T. Hirade et al., Application of an active control mount (ACM) for improved diesel engine vehicle quietness," *Application of an Active Control Mount (ACM) for Improved Diesel Engine Vehicle Quietness*, Technical Paper 1999-01-0832, SAE, Warrendale, PA, USA, 1999.

[57] Y. Nakaji, S. Satoh, T. Kimura, T. Hamabe, Y. Akatsu, and H. Kawazoe, "Development of an active control engine mount system," *Vehicle System Dynamics*, vol. 32, no. 2-3, pp. 185–198, 1999.

[58] C. Togashi and K. Ichiryu, "Study on hydraulic active engine mount," SAE, Warrendale, PA, USA, Technical Paper 2003-01-1418, 2003.

[59] C. Togashi, M. Nakano, and M. Nagai, "A study on active hydraulic engine mount to reduce interior car noise and vibration over wide frequency band," SAE, Warrendale, PA, USA, Technical Paper 2011-01-1636, 2011.

[60] H. Yuuske, H. Ryosuke, T. Chiharu et al., "Vibration control of the hydraulic active engine mount using a feedback controller with variable notch characteristics," in *Proceedings of the 2014 JSAE Annual Congress*, Springer, Pacifico Yokohama, Japan, May 2014.

[61] H. Matsuoka, T. Mikasa, and H. Nemoto, "NV countermeasure Technology for a cylinder-on-demand engine - development of active control engine mount," SAE, Warrendale, PA, USA, Technical Paper 2004-01-0413, 2004.

[62] Y. W. Lee, C. W. Lee, G. S. Jeong et al., "Modeling and dynamic analysis of active engine mount using electromagnetic actuator," in *Proceedings of the AVEC1996*, Swets & Zeitlinger, Aachen, Germany, June 1996.

[63] Y. W. Lee, C. W. Lee, G. S. Jeong et al., "Design of active engine mount and evaluation of vibration control performance using normalized filtered-X LMS algorithm," in *Proceedings of the Fourth International Conference on Motion and Vibration Control*, Wordware Publishing, Zurich, Switzerland, August 1998.

[64] C. W. Lee, Y. W. Lee, and B. R. Chung, "Performance test of active engine mount system in passenger car," in *Proceedings of Seventh International Congress on Sound and Vibration*, Garmisch-Partenkirchen, Germany, July 2000.

[65] Y.-W. Lee and C.-W. Lee, "Dynamic analysis and control of an active engine mount system," *Proceedings of the Institution of Mechanical Engineers, Part D: Journal of Automobile Engineering*, vol. 216, no. 11, pp. 921–931, 2002.

[66] B.-H. Lee and C.-W. Lee, "Model based feed-forward control of electromagnetic type active control engine-mount system," *Journal of Sound and Vibration*, vol. 323, no. 3-5, pp. 574–593, 2009.

[67] A. Gennesseaux, "A new generation of engine mounts," SAE, Warrendale, PA, USA, Technical Paper 951296, 1995.

[68] S. Jomaa, B. Thibault, and A. M. Clayton, "New two-step optimization process of an active engine mount: applying DFSS techniques and taguchi methods of robust design strategies: Part I," SAE, Warrendale, PA, USA, Technical Paper 2006-01-0279, 2006.

[69] N. Vahdati and S. Heidari, "Development of an electromagnetic active engine mount," in *Proceedings of the ASME 2015 International Mechanical Engineering Congress and Exposition*, ASME, Houston, USA, November 2015.

[70] S. Yasuki, Y. Asakai, H. Tashiro et al., "Development of new intelligent tourer 2004 model INSPIRE," *Review of Automotive Engineering*, vol. 16, no. 1, pp. 1–10, 2004.

[71] H. Mansour, S. Arzanpour, and F. Golnaraghi, "Design of a solenoid valve based active engine mount," *Journal of Vibration and Control*, vol. 18, no. 8, pp. 1221–1232, 2012.

[72] H. Mansour, S. Arzanpour, and M. Golnaraghi, "Active decoupler hydraulic engine mount design with application to variable displacement engine," *Journal of Vibration and Control*, vol. 17, no. 10, pp. 1498–1508, 2011.

[73] H. Mansour, "Design and development of active and semi-active engine mounts," Master's Thesis, Simon Fraser University, Burnaby, Canada, 2010.

[74] K. Sakamoto and T. Sakai, "Development of simulation model for active controlled engine mount," *Review of Automotive Engineering*, vol. 27, no. 1, pp. 155–157, 2006.

[75] K. Fumiya, K. Hirata, S. Masahiko et al., "Proposal of a two movers linear oscillatory actuator for active control engine mounts," *IEEE Transactions on Magnetics*, vol. 49, no. 5, pp. 2237–2240, 2013.

[76] K. Masashi, K. Hirata, and F. Kitayama, "Proposal of linear oscillatory actuator using DC motor for active control engine mount," *International Journal of Applied Electromagnetics & Mechanics*, vol. 52, no. 3, pp. 1–7, 2016.

[77] F. Kitayama, K. Hirata, and Y. Asai, "Study on active control engine mount with linear oscillatory actuator," in *Proceedings Of ISEF 2011 the 15th International Ymposium on Electromagnetic Fields in Mechatronics*, Electrical And Electronic Engineering, Funchal, Portugal, September 2011.

[78] H. Matsuoka, T. Misaka, and H. Nemoto, "Development of active control engine mount," *Honda R&D Technical Review*, vol. 15, no. 2, pp. 209–214, 2003.

[79] F. Kitayama, K. Hirata, N. Niguchi, and M. Kobayashi, "A new linear oscillatory actuator with variable characteristics using two sets of coils," *Sensors*, vol. 16, no. 3, pp. 377–385, 2016.

[80] F. Kitayama, K. Hirata, and T. Yamada, "Linear oscillatory actuator using new magnetic movement converter," in *Proceedings Of 2013 IEEE International Conference on Mechatronics and Automation*, IEEE, Takamatsu, Japan, pp. 431–436, September 2013.

[81] F. Kitayama, K. Hirata, M. Sakai, and T. Yoshimoto, "Linear oscillatory actuator using regenerative energy," *Journal of the Japan Society of Applied Electromagnetics and Mechanics*, vol. 21, no. 3, pp. 413–418, 2013.

[82] Y. Hasegawa and K. Hirata, "A study on electromagnetic actuator with two-degree-of-freedom," *IEEJ Transactions on Industry Applications*, vol. 125, no. 5, pp. 519–523, 2005.

[83] H. Katsuhiro, Y. Ichii, and Y. Arikawa, "Linear oscillatory actuator with dynamic vibration control," *IEEJ Transactions on Industry Applications*, vol. 122, no. 4, pp. 346–351, 2002.

[84] S. Arzanpour and M. F. Golnaraghi, "Development of a bushing with an active compliance chamber for variable displacement engines," *Vehicle System Dynamics*, vol. 46, no. 10, pp. 867–887, 2008.

[85] F. Hausberg, C. Scheiblegger, P. Pfeffer, M. Plöchl, S. Hecker, and M. Rupp, "Experimental and analytical study of secondary path variations in active engine mounts," *Journal of Sound and Vibration*, vol. 340, pp. 22–38, 2015.

[86] K. Seto, A. Nakamatsu, M. Ishihama et al., "Optimum design method for hydraulic engine mount (in Japanese)," SAE, Warrendale, PA, USA, Technical Paper 911055, 1991.

[87] G. Kim and R. Singh, "Nonlinear analysis of automotive hydraulic engine mount," *Journal of Dynamic Systems, Measurement, and Control*, vol. 115, no. 3, pp. 482–487, 1993.

[88] R. Singh, G. Kim, and P. V. Ravindra, "Linear analysis of automotive hydro-mechanical mount with emphasis on decoupler characteristics," *Journal of Sound and Vibration*, vol. 158, no. 2, pp. 219–243, 1992.

[89] J. E. Colgate, C.-T. Chang, Y.-C. Chiou, W. K. Liu, and L. M. Keer, "Modelling of a hydraulic engine mount focusing on response to sinusoidal and composite excitations," *Journal of Sound and Vibration*, vol. 184, no. 3, pp. 503–528, 1995.

[90] L. R. Miller and M. Ahmadian, "Active mounts- A discussion of future technological trends," in *Proceedings of the INTER-NOISE and NOISE-CON Congress and Conference*, Toronto, Canada, July 1992.

[91] A. Geisberger, A. Khajepour, and F. Golnaraghi, "Non-linear modelling of hydraulic mounts: theory and experiment," *Journal of Sound and Vibration*, vol. 249, no. 2, pp. 371–397, 2002.

[92] J. Christopherson and G. N. Jazar, "Optimization of classical hydraulic engine mounts based on RMS method," *Shock and Vibration*, vol. 12, no. 2, pp. 119–147, 2005.

[93] T. M. Lewis, "The effects of dynamic strain amplitude and static prestrain on the properties of viscoelastic materials," SAE, Warrendale, PA, USA, Technical Paper 911084, 1991.

[94] M. Tiwari, H. Adiguna, and R. Singh, "Experimental characterization of a nonlinear hydraulic engine mount," *Noise Control Engineering Journal*, vol. 51, no. 1, pp. 36–49, 2003.

[95] A. R. Payne, "The dynamic properties of carbon black-loaded natural rubber vulcanizates. Part I," *Journal of Applied Polymer Science*, vol. 6, no. 19, pp. 57–63, 1962.

[96] H. Scher, M. F. Shlesinger, and J. T. Bendler, "Time-scale invariance in transport and relaxation," *Physics Today*, vol. 44, no. 1, pp. 26–34, 1991.

[97] J. C. Maxwell, "On the dynamical theory of gases," *Proceedings of the Royal Society of London*, vol. 15, pp. 167–171, 1867.

[98] M. A. Meyers and K. K. Chawla, *Mechanical Behaviors of Materials*, Prentice-Hall, Upper Saddle River, NJ, USA, 1999.

[99] P. K. Wong, Z. C. Xie, Y. C. Cao et al., "Design and optimization on active engine mounting systems for vibration isolation," *Applied Mechanics and Materials*, vol. 479-480, pp. 202–209, 2014.

[100] P. H. Lee, B. H. Lee, and C. W. Lee, "Design of an active control engine mount using a direct drive electrodynamic actuator," in *Proceedings of the 2007 ASME International Design Engineering Technical Conferences and Computers and Information in Engineering Conference*, ASME, Las Vegas, NV, USA, September 2007.

[101] Z. C. Xie, P. K. Wong, C. Cao et al., "A numerical investigation on active engine mounting systems and its optimization," *Journal of Vibroengineering*, vol. 16, no. 7, pp. 3273–3280, 2014.

[102] Y.-H. Shin, S.-J. Moon, J.-M. Kim, H.-Y. Cho, J.-Y. Choi, and H.-W. Cho, "Design considerations of linear electromagnetic actuator for hybrid-type Active mount damper," *IEEE Transactions on Magnetics*, vol. 49, no. 7, pp. 4080–4083, 2013.

[103] J.-Y. Park and R. Singh, "Analysis of powertrain motions given a combination of active and passive isolators," *Noise Control Engineering Journal*, vol. 57, no. 3, pp. 232–243, 2009.

[104] C. Scheiblegger, J. Lin, and H. Karrer, "New nonlinear bushing model for ride comfort and handling simulation: focussing on linearization and the implementation into MBS environment," *Lecture Notes in Electrical Engineering*, vol. 198, pp. 461–473, 2013.

[105] P. Pfeffer and K. Hofer, "Simple non-linear model for elastomer and hydro-mountings to optimise overall vehicle simulation," *ATZ Worldwide*, vol. 104, no. 5, pp. 5–7, 2002.

[106] C. Scheiblegger, N. Roy, O. Silva Parez et al., "Non-linear modeling of bushings and cab mounts for calculation of durability loads," SAE, Warrendale, PA, USA, Technical Paper 2014-01-0880, 2014.

[107] C. Scheiblegger, "Modelling of elastomer and hydro mounts for ride comfort and handling simulation," in *Proceedings of the 3rd PhD Symposium of Minich University of Applied Sciences*, Munich, Germany, June 2015.

[108] S. Lambertz, *Nichtlineares Materialgesetz für technische Gummiwerkstoffe mit deformationsabhängigen eigenschaften und seine experimentelle Überprüfung an gummifederelementen (Berichte aus der Werkstofftechnik)*, PhD Thesis, Shaker, Aachen, Germany, 1993.

[109] A. A. Wijaya, F. J. Darsivan, M. I. Solihin et al., "Terminal sliding mode control for active engine mounting system," in *Proceedings of the 2009IEEE/ASME International Conference On Advanced Intelligent Mechatronics*, IEEE, Singapore, July 2009.

[110] V. Fakhari, A. Ohadi, and H. A. Talebi, "A robust adaptive control scheme for an active mount using a dynamic engine model," *Journal of Vibration and Control*, vol. 21, no. 11, pp. 2223–2245, 2013.

[111] S. M. Kuo and D. M. Morgan, *Active Noise Control Systems: Algorithms and DSP Implementation*, John Wiley & Sons, New York, NY, USA, 1996.

[112] C. H. Hansen and S. D. Snyder, *Active Control of Noise and Vibration*, E & FN Spon, London, UK, 1997.

[113] R. L. Clark, W. R. Saunders, and G. P. Gibbs, *Adaptive Structures: Dynamics and Control*, John Wiley & Sons, New York, NY, USA, 1998.

[114] S. J. Elliott, *Signal Processing for Active Control*, Academic Press, London, UK, 2001.

[115] M. Bernuchon, "A new generation of engine mounts," SAE, Warrendale, PA, USA, Technical Paper 840259, 1984.

[116] C. Olsson, "Active automotive engine vibration isolation using feedback control," *Journal of Sound and Vibration*, vol. 294, no. 1, pp. 162–176, 2006.

[117] B. Riley, M. Bodie, J. Hoying et al., "Active vibration and noise cancellation control of four-cylinder engines – an application," SAE, Warrendale, PA, USA, Technical Paper 951299, 1995.

[118] J. M. Yang, Y. Suematsu, and Z. Kang, "Two-degree-of-freedom controller to reduce the vibration of vehicle engine-body system," *IEEE Transactions on Control Systems Technology*, vol. 9, no. 2, pp. 295–304, 2001.

[119] A. J. Hillis, S. A. Neild, D. P. Stoten et al., "A minimal controller synthesis algorithm for narrow-band Applications," *Proceedings of the Institution of Mechanical Engineers, Part I: Journal of Systems and Control Engineering*, vol. 219, no. 8, pp. 591–607, 2005.

[120] B. Seba, N. Nedeljkovic, J. Paschedag, and B. Lohmann, "H∞ Feedback control and Fx-LMS feedforward control for car engine vibration attenuation," *Applied Acoustics*, vol. 66, no. 3, pp. 277–296, 2005.

[121] W. K. Shi and J. Cai, "A study of the isolation characteristics of an active control hydraulic mount with electromagnetic-actuator," *Noise and Vibration Control*, vol. 26, no. 3, pp. 1–5, 2006.

[122] H. R. Karimi and B. Lohmann, "Haar wavelet-based robust optimal control for vibration reduction of vehicle engine–body system," *Electrical Engineering*, vol. 89, no. 6, pp. 469–478, 2007.

[123] K. K. Shin, "Active vibration control of active fuel management engines using active engine mounts," in *Proceedings of the ASME 2007 International Mechanical Engineering Congress and Exposition*, ASME, Washington, DC, USA, November 2007.

[124] F. J. Darsivan, W. F. Faris, and W. Martono, "Active engine mounting controller using extended minimal resource allocating networks," *International Journal of Vehicle Noise and Vibration*, vol. 4, no. 2, pp. 3–12, 2008.

[125] F. J. Darsivan, W. F. Faris, and W. Martono, "Active engine mounting control algorithm using neural network," *Shock and Vibration*, vol. 16, no. 4, pp. 417–437, 2009.

[126] V. Fakhari, H. A. Talebi, and A. R. Ohadi, "A robust active vibration control of automotive engine," in *Proceedings of the Asme Biennial Conference on Engineering Systems Design & Analysis 2010*, Istanbul, Turkey, July 2010.

[127] A. J. Hillis, "Multi-input multi-output control of an automotive active engine mounting system," *Proceedings of the*

Institution of Mechanical Engineers Part D Journal of Automobile Engineering, vol. 225, no. 11, pp. 1492–1504, 2011.
[128] A. M. Mahil, M. A. Shah, and W. F. Faris, "Active engine mounting controller design using linear quadratic regulator and proportional integral derivative," *International Journal of Automation and Control*, vol. 5, no. 3, pp. 284–297, 2011.
[129] S. C. Fok, M. W. S. Lau, G. L. Seet, and E. Low, "Active force cancellation of a near resonance vibrating system using robust H," *International Journal of Vehicle Noise and Vibration*, vol. 8, no. 1, pp. 36–50, 2012.
[130] V. Fakhari and A. Ohadi, "Robust control of automotive engine using active engine mount," *Journal of Vibration and Control*, vol. 19, no. 7, pp. 1024–1050, 2012.
[131] A. Raoofy, V. Fakhari, and A. R. Ohadi Hamedani, "Vibration control of an automotive engine using active mounts," *The Journal of Engine Research*, vol. 30, pp. 03–14, 2013.
[132] G. C. Sun, C. H. Zhang, and H. Xin, "Active engine vibration isolation using robust control," *Applied Mechanics and Materials*, vol. 380–384, pp. 504–507, 2013.
[133] C. Bao, P. Sas, and H. V. Brussel, "Comparison of two on-line identification algorithms for active noise control," in *Proceedings of the 2nd Conference on Recent Advances in Active Control of Sound and Vibration*, Blacksburg, Blacksburg, USA, January 1993.
[134] F. Hausberg, S. Hecker, P. Pfeffer et al., "Incorporation of adaptive grid-based look-up tables in adaptive feedforward algorithms for active engine mounts," in *Proceedings of the International Symposium on Advanced Vehicle Control*, ISSN, Tokyo, Japan, September 2014.
[135] V. Fakhari, S. B. Choi, and C. H. Cho, "A new robust adaptive controller for vibration control of active engine mount subjected to large uncertainties," *Smart Materials & Structures*, vol. 24, no. 4, pp. 1–11, 2015.
[136] R. Guo, X. K. Wei, and J. Gao, "An improved PID controller based on particle swarm optimization for active control engine mount," SAE, Warrendale, PA, USA, Technical Paper 2017-01-1056, 2017.
[137] R. Guo, X. K. Wei, and J. Gao, "Extended filtered-x-least-mean-squares algorithm for an active control engine mount based on acceleration error signal," *Advances in Mechanical Engineering*, vol. 9, no. 9, pp. 1–11, 2017.
[138] F. J. Darsivan, *Active engine mounting system based on neural network control*, PhD Thesis, IIUM, Malaysia, 2010.
[139] A. Hosseini, "A solenoid-based active hydraulic engine mount: modelling, analysis, and verification," Master's Thesis, Simon Fraser University, British Columbia, Canada, 2010.
[140] S. J. Elliott, I. Stothers, and P. A. Nelson, "A multiple error LMS algorithm and its application to the active control of sound and vibration," *IEEE Transactions on Acoustics, Speech, and Signal Processing*, vol. 35, no. 10, pp. 1423–1434, 1987.
[141] S. M. Kou and D. R. Morgan, "Active noise control, a tutorial review," *Proceedings of the IEEE*, vol. 87, no. No. 6, pp. 943–973, 1999.
[142] J. J. Shynk, "Frequency-domain and multirate adaptive filtering," *IEEE Signal Processing Magazine*, vol. 9, no. 1, pp. 14–37, 1992.
[143] L. Ljung, *System Identification: Theory for the User*, Prentice Hall PTR, Englewood Cliffs, New Jersey, 1999.
[144] P. V. Overschee and B. D. Moor, *Subspace Identification of Linear Systems: Theory, Implementation, Applications*, Springer, Berlin, Germany, 1996.
[145] A. M. M. Mahil and W. F. Faris, "Modelling and control of four and six DOF active engine mount system using (PID and LQR)," *International Journal of Vehicle Noise and Vibration*, vol. 10, no. 4, pp. 326–349, 2014.
[146] C. Olsson, *Active engine vibration isolation using feedback control*, PhD Thesis, Link€opings Universitet, Linköping, Sweden, 2002.
[147] B. Widrow and M. E. Hof, "Adaptive switching circuits," *Re Wescon Convention Record*, vol. 96-104, 1960.
[148] W. B. Conover, "Fighting noise with noise," *Noise Control*, vol. 2, no. 2, pp. 78–92, 1956.
[149] D. R. Morgan, "An analysis of multiple correlation cancellation loops with a filter in the auxiliary path," *IEEE Transactions on Acoustics, Speech, and Signal Processing*, vol. 28, no. 4, pp. 454–467, 1980.
[150] R. Fraanje, S. J. Elliott, and M. Verhaegen, "Robustness of the filtered-X LMS algorithm— Part II: robustness enhancement by minimal regularization for norm bounded uncertainty," *IEEE Transactions on Signal Processing*, vol. 55, no. 8, pp. 4038–4047, 2007.
[151] R. Fraanje, M. Verhaegen, and N. Doelman, "Increasing the robustness of a preconditioned filtered-X LMS algorithm," *IEEE Signal Processing Letters*, vol. 11, no. 2, pp. 285–288, 2004.
[152] A. P. Berkhoff, "A technique for improved stability of adaptive feedforward controllers without detailed uncertainty measurements," *Applied Geomatics*, vol. 21, no. 6, pp. 371–378, 2012.
[153] F. Hausberg, S. Vollmann, P. Pfeffer et al., "Improving the convergence behavior of active engine mounts in vehicles with cylinder-on-demand engines," in *Proceedings of the International Congress and Exposition on Noise Control Engineering*, Innsbruck, Austria, September 2013.
[154] D. P. Stoten and S. A. Neild, "The error-based minimal control synthesis algorithm with integral action," *Journal of Systems and Control Engineering, Part I, Mechanical Engineering*, vol. 217, pp. 187–201, 2003.
[155] P. A. Ioannou and J. Sun, *Robust Adaptive Control*, PTR Prentice-Hall, New York, NY, USA, 1996.
[156] B. Yao and M. Tomizuka, "Smooth robust adaptive sliding mode control of manipulators with guaranteed transient performance," in *Proceedings of 1994 American Control Conference*, Baltimore, USA, July 1994.
[157] K. K. Shin, "Integrated open and closed-loop control method for active engine mounts," US Patent Application No. 7974769, 2011.